CHAPTER 2

TRICHLOROACETIC ACID IMPRINTED POLYMER AND PIEZOELECTRIC QUARTZ CRYSTAL MICROBALANCE TRANSDUCER

2.1. Principle of piezoelectric quartz crystal microbalance transducer (Mecea, 2005)

Piezoelectric quartz crystal microbalance (QCM) is one of the popular transducers among the biosensing methods. Owing to its simplicity, convenience, low economical cost and quick real-time response, QCM has been utilized in many fields including food analysis, clinical analysis, environmental monitoring and gene probe assay. The principle of the QCM detection relies on the recording of frequency decrease corresponding to mass increase on the chip surface during the biological interactions. However, the quantitative relationship was not established until 1959. The possibility of using quartz crystal resonators as quantitative mass measuring devices was first explored by Sauerbrey. The decrease of the resonant frequency of a thickness shear vibrating quartz crystal resonator, having AT or BT cut, was found to be proportional to the added mass of the deposited film according to the equation as shown below:

$$\Delta f = \frac{f_q^2 M_f}{N \rho_q S} = \frac{f_q^2 m_f}{N \rho_q} \qquad (2\text{-}1)$$

where f_q is the fundamental resonant frequency of the quartz, N is the frequency constant of the specific crystal cut (N_{AT} = 1.67 x 105 Hz . cm; N_{BT} = 2.5 x 105 Hz . cm), ρ_q = 2.65 kg dm^{-3} is the quartz density, and S is the surface area of the deposited film, the mass of which is M_f. When the deposited film covers the whole sensitive area of the quartz resonator, it is better to use the real density, $m_f = M_f/S$, to further calculate the film thickness, $l_f = m_f/\rho_f$, where ρ_f is the density of the deposited film. A typical quartz crystal resonator is shown in Fig. 2.1. The keyhole-shaped electrodes on both major faces of the quartz resonator are vacuum deposited gold or silver films, about 150 nm thick. The mass-sensitive area is situated in the central part of the resonator, covering the area where the two electrodes overlap. Equation (2-1) shows the QCM mass sensitivity, where D_f/m_f is proportional to the square of the quartz resonator frequency.

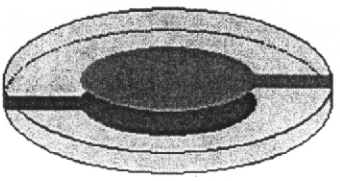

Fig. 2.1. A typical quartz crystal resonator used for mass measurements. (Mecea, 2005)

There are experimental data showing mass sensitivity distribution on the surface of a quartz crystal resonator that closely follows the vibration amplitude distribution. The recorded frequency change of deposited silver spots, which have the same mass, M_f, is proportional to the vibration amplitude indicated by the voltage, U. A 5 MHz, plano-convex, AT-cut resonator with 200 mm curvature radius was used. The diameter of the resonator was 14 mm. It had silver electrodes of different diameters on each side: 13 mm on the flat side and 6 mm on the convex side. To reveal the mass sensitivity distribution, small silver spots having the same thickness and a diameter of 0.6mm were vacuum deposited along one of the crystal diameters, with 0.5 mm spacing between them. The amplitude distribution along the same diameter was revealed by using the scanning probe method. The voltage, U, is proportional to the vibration amplitude at each point along the directional diameter. Both the mass sensitivity and amplitude distribution curve follow a Gaussian function. The displacement of a point, vibrating with simple harmonic motion, could be described as

$$x = A\sin(\omega t) \tag{2-2}$$

where A is the vibrational amplitude and $\varpi = 2\pi f$ is the angular frequency. The acceleration of this motion is

$$a = -\omega^2 A\sin(\omega t) = -4\pi^2 f^2 A\sin(\omega t) \tag{2-3}$$

The maximum value of the acceleration in that point is $a_{max} = \omega^2 A$. On the crystal surface the highest vibration amplitude, A_0, and the maximum acceleration, $a_0 = \omega^2 A_0$, are in the center of the quartz resonator.

From Eq. (2-1), the mass measuring sensitivity is proportional to the square of the quartz resonator frequency. From the experimental results shown in Fig. 2.2, the mass measuring sensitivity of the QCM is proportional to the vibrating amplitude at that point (Mecea, 2005).

These two statements lead to the conclusion that the physical quantity that determines the mass measuring sensitivity in every point on the surface of a quartz crystal resonator is the acceleration of the crystal vibration in that point.

Piezoelectric quartz crystal microbalance is a passive solid-state electronic device which can respond to changes in temperature, pressure, and most importantly, to changes in physical properties at the interface between the device surface and a foreign fluid or solid. Such changes in physical properties include variations in interfacial mass density, elasticity, viscosity, and layer thickness. The incorporation of various chemically sensitive layers has enabled the transition from the microbalance to the mass sensor and resulted in the explosive growth of piezoelectric sensors in recent years.

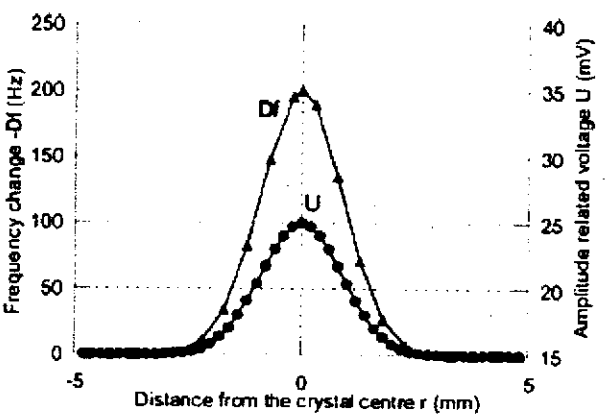

Fig. 2.2. Mass sensitivity related D_f and vibration amplitude related U distribution along one of the quartz resonator diameters (Mecea, 2005).

This type of transducer operates by observation of the propagation of an acoustic wave through the solid-state device. Sensing is achieved by correlating acoustic wave propagation variations to the amount of analyte captured at the surface and then to the amount or concentration of analyte present in the sample exposed to the sensor, or to the changes of physical properties of interfacial thin films.

Measurement of the frequency shift and resonant resistance change of acoustic wave is one of the most accurate types of physical measurement. The frequency and resonant resistance of piezoelectric crystal is influenced by a large number of parameters mentioned above. A selective sensor is obtained when a sensor surface is coated with selective interacting thin film.

To implement a QCM biosensor, the source compound has to be immobilized on the crystal surface to capture the target compound. It is crucial to obtain an appropriate immobilization approach to ensure high sensitivity and stability response in practical QCM applications.

2.2. Trichloroacetic Acid Imprinted Poly(Ethyleneglycoldimethacrylate-*co*-4-vinylpyridine) Modified Quartz Crystal Microbalance Sensor

2.2.1. Objective

To assess the feasibility of using a copolymer of ethylene glycol methacrylate and 4-vinylpyridine imprinted with a chlorinated by-product trichloroacetic acid as a recognition material of haloacetic acids in a mass sensitive quartz crystal microbalance sensor.

2.2.2. Method

2.2.2.1. Immobilisation of a polymer on a QCM electrode

To prepare a QCM electrode, a dual QCM-pattern was sequentially screen printed on each side of 10 MHz AT-cut quartz disc (15 mm diameter), using the gold screen-printing technique. The electrode facing the aqueous phase had a diameter of 4.5 mm with 2.5 mm electrode on the gas-phase side (Fig 2.3a). The thickness of the gold electrode layer on each side of the quartz crystal after sintering was determined to be about 180 nm, by scratching with a needle and measuring depth of the scratches using an AFM with a Nanotec Electrinica WSxM scanning probe microscopy software version 3.0 Beta 8.1. The procedure for immobilization of MIP on electrodes was as follows: 14 mg of TCAA (0.08 mmol), 34 mg of VPD (0.32 mmol), 200 mg of EDMA (1.0 mmol) and 9 mg of AIBN (0.05 mmol) were dissolved in 1 ml of acetonitrile. Then, the solution was purged with a stream of nitrogen gas for 1 min, and pre-polymerization was carried out in a water bath at 65 ^{o}C for 1 min. The non-imprinted polymer (NIP) was prepared in the same manner as the MIP, but in the absence of the TCAA template. The crystal was spin-coated with 10 μl of the MIP solution onto the center of the surface of the

analytical electrode with a rotation speed of 3000 rpm, followed by spin-coating of 10 µl of the NIP solution at the reference electrode. Subsequently, the blank quartz was placed in a chamber flushed with nitrogen gas for 1 min. Polymerisation was carried out in a hot-air oven at 70 ^{O}C for 18 h. After the immobilizing process, the electrode was washed with five portions of 100 ml de-ionized water to remove the template molecules. For removing the templates absorbed in the recognition sites, a washing process in de-ionized water was needed for at least 3 h. Finally, the electrode was dried in air for overnight. The thickness of the MIP coated films was inspected using an AFM method that was similar to the method employed for measuring the gold layer onto electrodes.

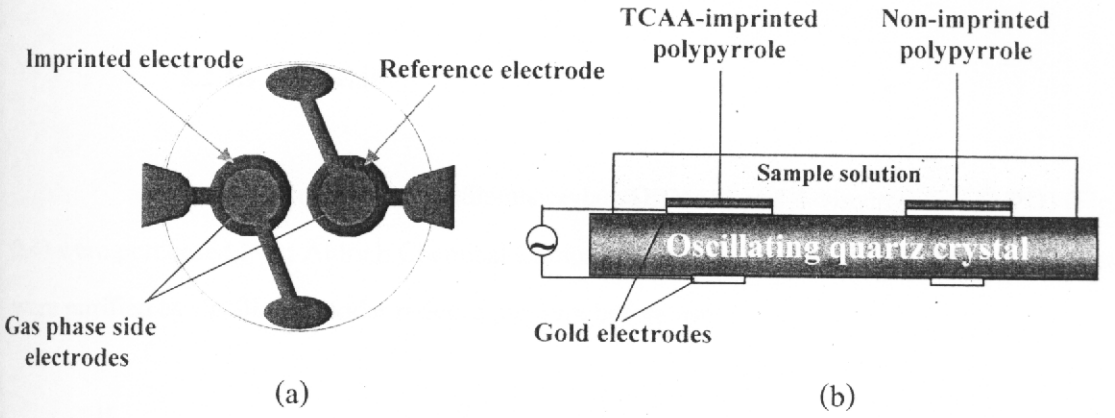

Fig. 2.3. (a) QCM electrodes geometry, (b) QCM electrodes fabricated in measuring flow cell

2.2.2.2. Fabrication of the sensor device

A QCM constructed with a coated TCAA-MIP and a corresponding coated NIP gold electrode was mounted in a flow-cell (Fig. 2.3b) with a volume of 250 µl and placed in a thermostat at 25 ^{O}C. A home-built oscillator circuit and a self-programmed frequency read-out were used with a processing software. The oscillator frequency was measured by means of a frequency counter. The responses of the oscillator circuit were checked by means of a network analyser to obtain data relating to acoustic damping and frequency shifts. The sensor experiments were performed using a flow system with a flow rate of 2 ml min^{-1}. Before making a measurement, the sensor was stabilized by running 200 ml de-ionized water through the cell for 3

h. One hundred milliliters of a series of standard solutions of TCAA and analogs were run through the cell separately. The frequencies of both TCAA-MIP-QCM and the corresponding NIP-based QCM were recorded as parallel until a stable frequency was obtained. The water samples were analysed under the same conditions as those used for the standard solutions. For the sample measurement using the sensor, the response of the sensor exposed to a solution of the analyte was reported as a frequency shift response ($-\Delta F$), which was a difference value of the frequency shift of the MIP electrode and the frequency shift of the NIP electrode. All measurements were performed in triplicate.

2.2.3. Material and equipment

2.2.3.1. Material

Ethylene glycol dimethacrylate (EDMA) and 4-vinylpyridine (VPD) (Fig. 2.4) were purchased from Aldrich Chemical Company (Mil-waukee, WI, USA). These chemicals were purified by distillation under reduced pressure before use.

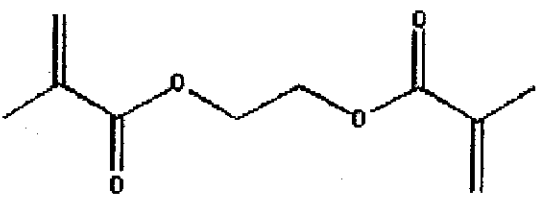

Ethylene glycol dimethacrylate (EDMA) cross-linker

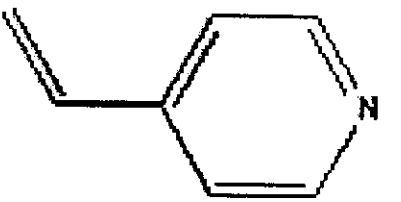

4-Vinylpyridine (VPD) functional monomer

Fig. 2.4. Cross-linker and functional monomer used to prepare acrylate type polymer

2,2-Azobis-(isobutyronitrile) (AIBN) was obtained from Janssen Chimica (Geel, Belgium) and its molecular structure is shown below (Fig. 2.5)

Polydimethyl-siloxane and hardener (Sylgard 184) were obtained from Dow Corning Corporation (MI, USA).

Trichloroacetic acid (TCAA) was purchased from Merck K.G. (Darmstadt, Germany). Dichloroacetic acid (DCAA), monochloroacetic acid (MCAA), tribromoacetic acid (TBAA), dibromoacetic acid (DBAA), monobromoacetic acid (MBAA), and malonic acid were obtained from Fluka Chemie AG (Buchs, Switzerland).

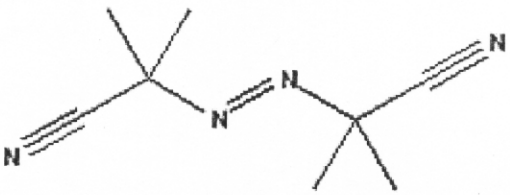

Fig. 2.5. 2,2-Azobis-(isobutyronitrile) initiator used in the polymerization process

2.2.3.2. Equipment

Ismatec peristaltic pump (MCP-Process Series, Ismatec SA, Wertheim-Mondfeld, Germany) was used to drive the sample solution into the flow cell (Fig. 2.6).

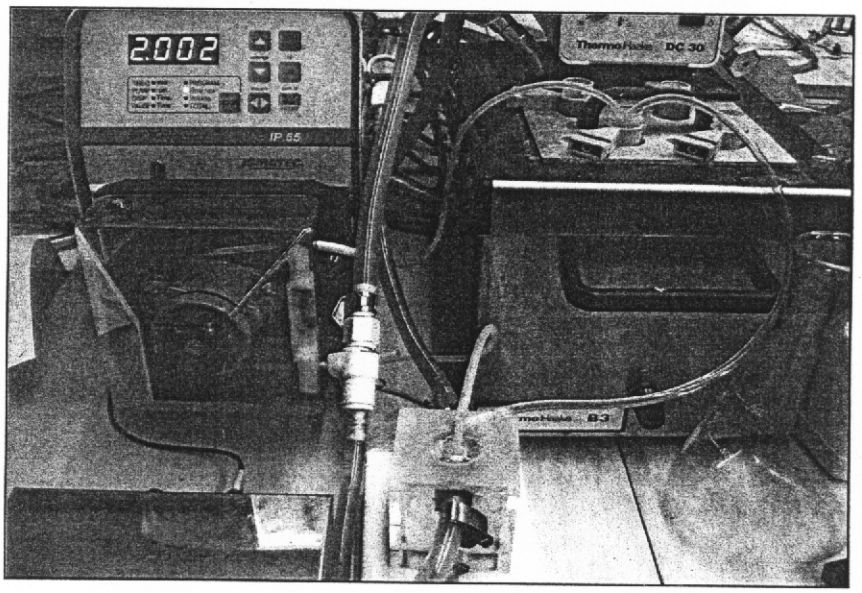

Fig. 2.6. MCP-Process Series Ismatec peristaltic pump

An RF network analyser (8712ET 300 KHz-1300 MHz, Agilent Technologies, Palo Alto, CA) (Fig. 2.7) was utilized to monitor output signals which read the resistance signals from the sensor array with subsequent display on the Laptop screen.

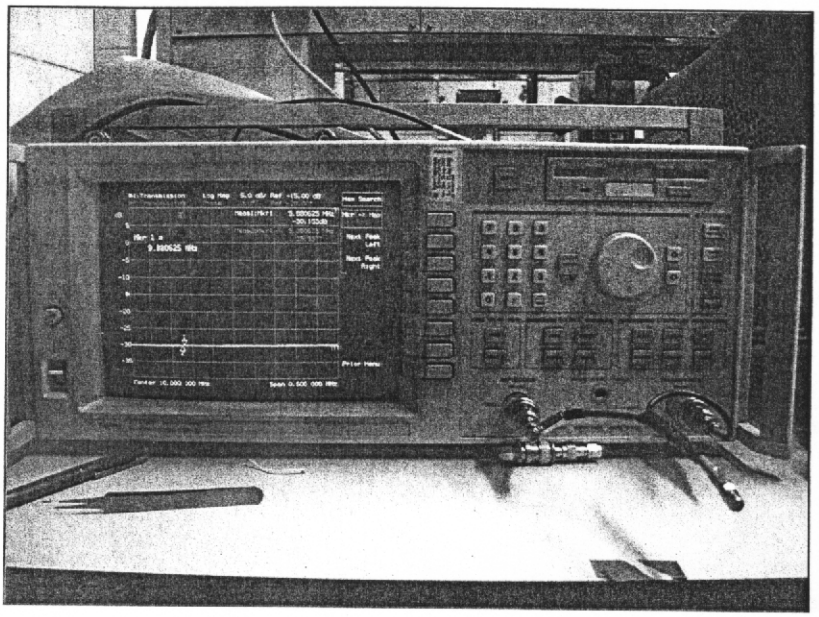

Fig. 2.7. 8712ET RF network analyzer

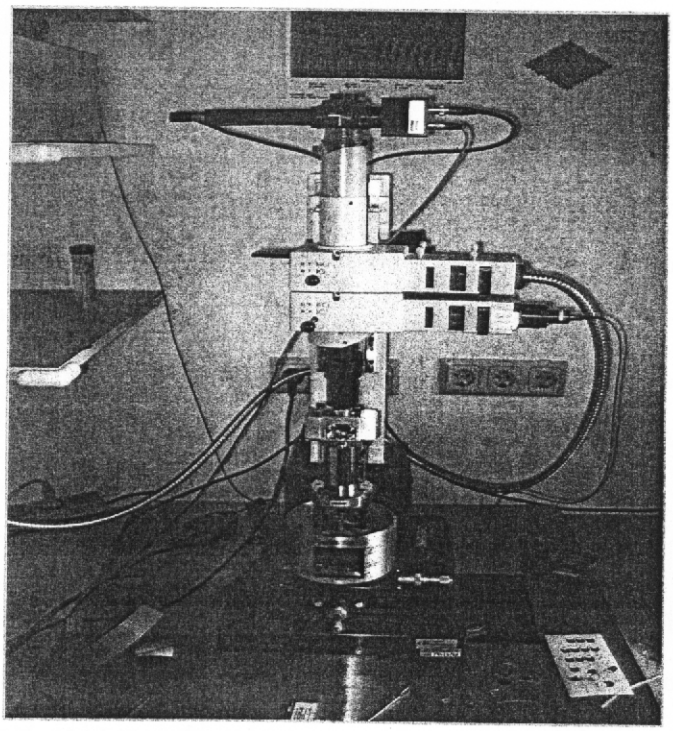

Fig. 2.8. Atomic force microscope (AFM)

An atomic force microscope (AFM) (Digital Instru-ments Inc., Santa Barbara, CA) (Fig. 2.8) using a Nanoscope III Scanning tunnel microscope was used to inspect

the morphology of the deposited film. An AFM (Digital Instruments, CA, USA) with a Nanotec Electrinica WSxM scanning probe microscopy software version 3.0 Beta 8.1 (Digital Instruments, CA, USA) was utilized to determine the thickness of the films scratching with a needle and measuring depth of the scratches.

2.2.4. Results and discussion

2.2.4.1. The influence of the polymer composition on performance of the TCAA-MIP-QCM sensor

Recently, the combination of a QCM based on microgravimetric measurements and an MIP has been applied in selective sensing detection. Owing to MIP can be easily integrated on a transducer surface with several techniques. Typically, the thickness of the MIP layer located on a sensor surface is a very important factor in determining sensor's sensitivity. Thus, a thin or an ultra thin film of an MIP should be produced in order to acquire a sensitive sensor. A certain group of film producing theme has been reported varying in thickness of MIP fabricated. In situ electro-polymerisation was principally applied for the electrochemical MIP; physical entrapment of MIP particles into gel; or chemical coupling of the MIP has been used scarcely. A spin-coating method was chosen to immobilize the MIP onto the QCM electrode for this work. Because of this method can produce a MIP film in a required nanometer range.

A TCAA-imprinted cross-linked poly(VPD-*co*-EDMA) has been prepared by copolymerization of a VPD functional monomer and a high mole ratio of EDMA cross-linker in the presence of a TCAA template in acetonitrile. As can be seen in Fig. 2.9, the highest frequency shift response to 100 mg l^{-1} of the TCAA was observed when using 1:4 mole ratio of TCAA:VPD. This may be because a good recognition site should be constituted of a functional group from functional monomer behave as a driving force to attract the template molecule to the site and subsequent screening the molecule by the shape and size of cavity. Although, the interaction between the functional monomer and the template should be 1:1 mole ratio theoretical considering from their available function group. Actually, complete encounter of functional monomer to template to form complex is impossible. To increase the possibility of the functional

monomer's forming a complex with template, the excess amount of the functional group needed to be employed. And this 1:4 mole ratio of template:monomer may be the ratio at which the possibility of the functional monomer's interacting with the template was the highest. Additionally, to find a suitable rigidity of a polymer having a good recognition property and stability, the effect of the cross-linker amount was also investigated and can be seen in Fig. 2.10.

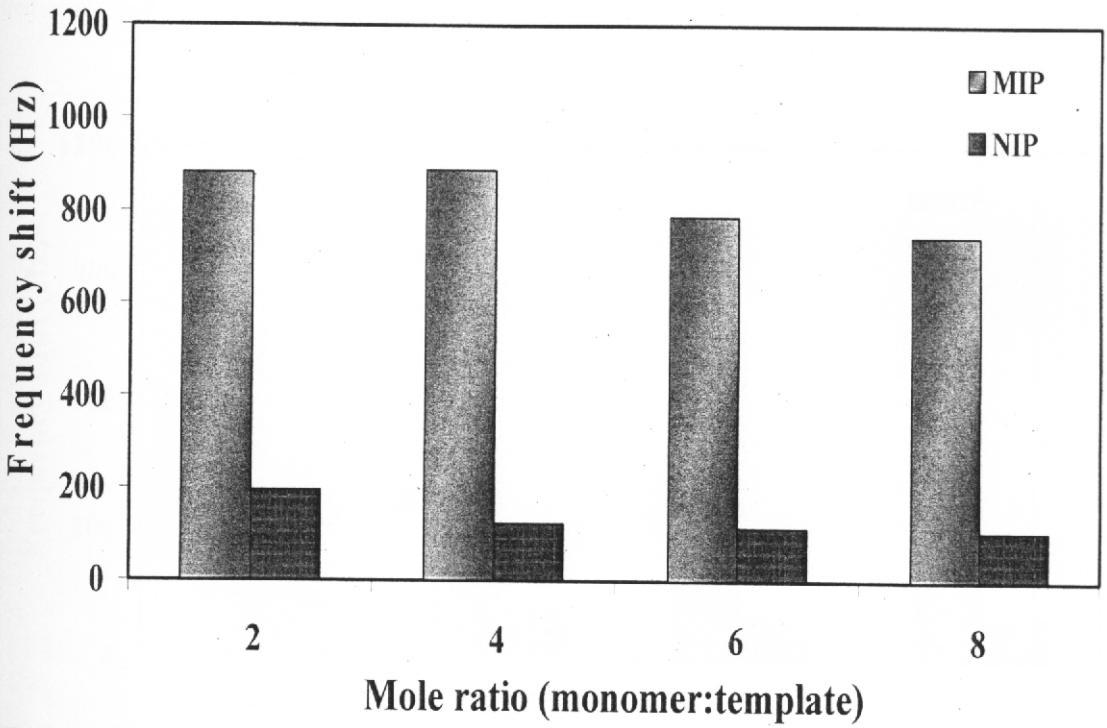

Fig. 2.9. Effect of the functional monomer-template mole ratio of the copoly(VPD-EGDMA) on the frequency shift of the polymer-coated QCM electrode prepared by using 85 % of the EDMA cross-linker

It was found that when using 85% of the cross-linker to prepare a polymer layer, the frequency difference between the MIP and the NIP after washing was the highest. It was presumably due to the cross-linker structure contributed to rigidity of polymer. A suitable rigidity should have a good binding site, since, the lower rigidity of structure produced a more easily changed binding site from environmental factors, and the higher rigidity of structure inhibited the inclusion of the template through the dense network. After verifying the optimized polymer composition, such optimized mole ratio of TCAA:VPD:EDMA was used to prepare a polymer layer coated on the electrode surface. This polymer composition not only showed a good

molecular recognition, comparing to that of the other TCAA:VPD:EDMA mole ratios (1:2:12, 1:6:12, 1:8:12, 1:4:10, 1:4:15 and 1:4:18), but also generated a film on gold electrode surfaces with a good adhesion stability. The low relative standard deviation (2.4%, n = 4) suggested a good and reproducible coating. Many environmental interferences, such as viscosity, conductivity, pressure fluctuations, and vibration of the system during the measurement, were compensated by a reference electrode coated with the NIP which was concurrently measured the frequency shift with the MIP electrode.

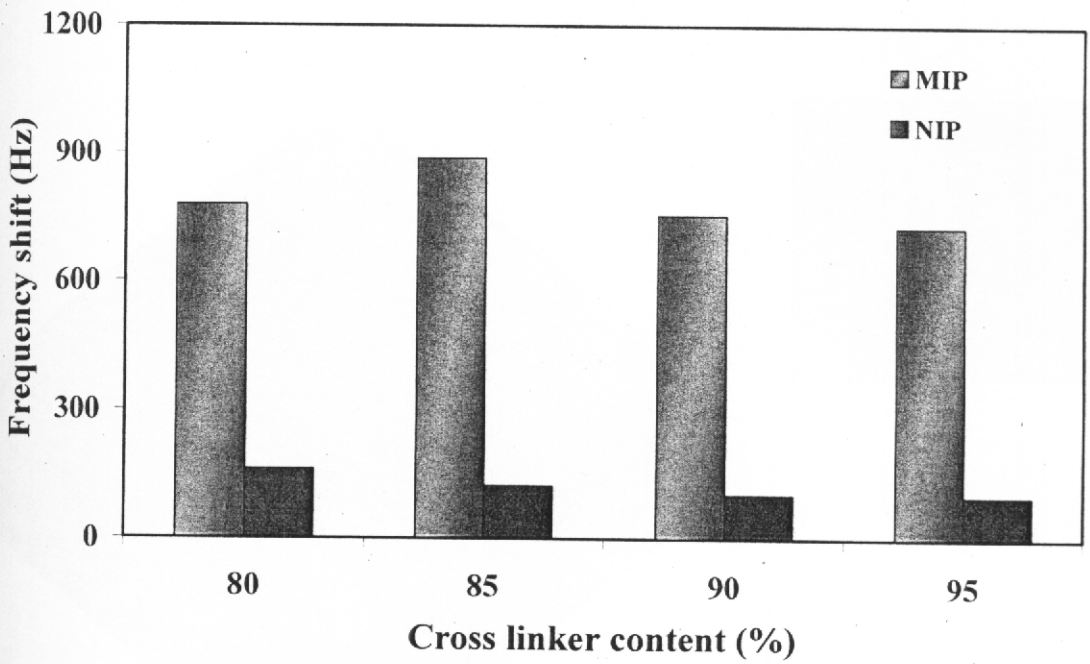

Fig. 2.10. Effect of the cross-linker content of the copoly(VPD-EGDMA) on the frequency shift of the polymer-coated QCM electrode prepared by using 1:4 mole ratio of TCAA:VPD

2.2.4.2. The effect of the coated polymer layer height on the frequency shift of the TCAA-MIP-QCM sensor

The coated thickness of the polymer layer on the electrode surface was approximately evaluated through the mass change-frequency shift relationship based on the Sauerbrey equation as can be seen below. The difference in frequency shift (ΔF) of the QCM electrode before and after the MIP immobilization was found to be 0.0196±0.0004 Hz, which

corresponded to about 800 nm (Smith and Shirazi, 2005) with calculation using the equation parameters manifested in the next paragraph.

$$\Delta f = \frac{f_0^2 \Delta m}{N \rho_q A} \tag{2-4}$$

where f_0 is the fundamental frequency of the crystal, N the modulus of the quartz (167 kHz cm), ρ_q the quartz density (2.648 g cm^{-3}), and A is the piezoelectrically active area. The film thickness of the polymer acquired by the QCM had good agreement with that obtained by the AFM method (Fig. 2.11).

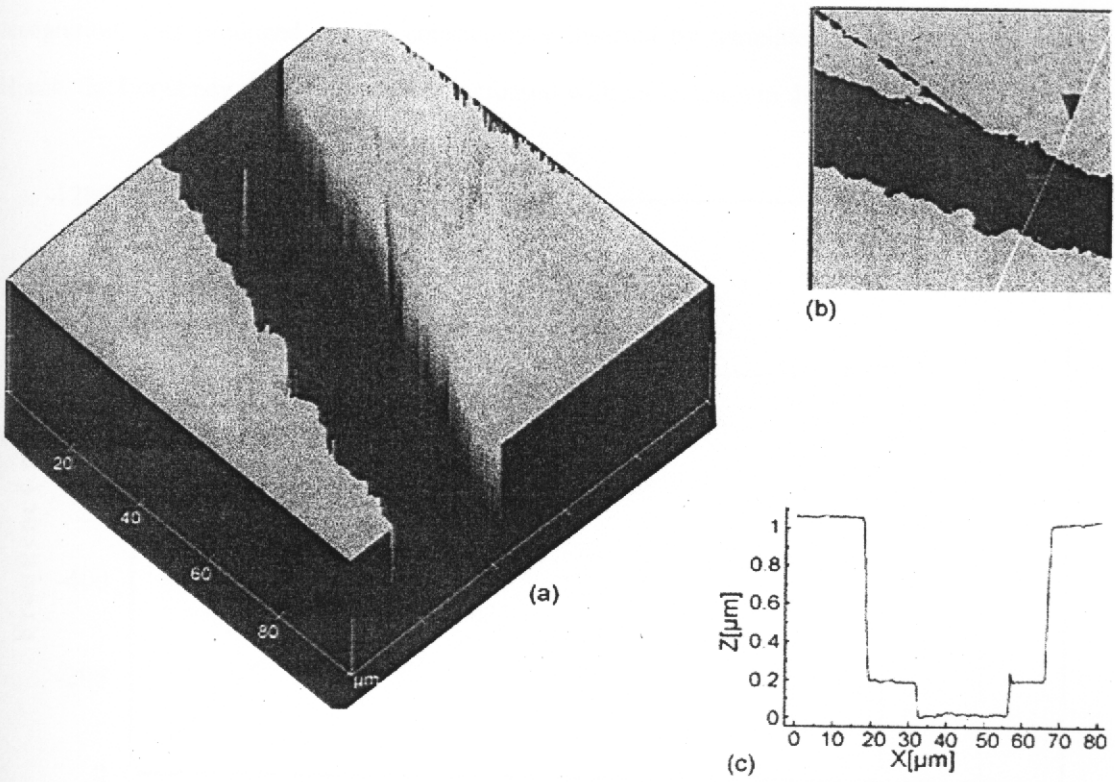

Fig. 2.11. (a) AFM 3D topography; (b) AFM of a cross-section of a scratch on a 20 kHz-MIP layer, and the measured depth of the polymer layer of 870 nm which is shown on (c) the plot of depth (z) vs. width (x) generated using the Nanotec Electrinica WSxM scanning probe microscopy software version 3.0 Beta 8.1. Scan rate of 1000 Hz is used.

A series of TCAA-imprinted polymers with various layer thicknesses was prepared at 1:4:12 TCAA/VPD/EDMA molar ratio and their layer heights were preliminarily evaluated by the AFM machine. The bulk effects of the layer on the frequency shift of the sensor were subsequently performed by the QCM measurement. When using 100 mg l^{-1} (ppm) TCAA as a solution sample, the different thickness of the imprinted layer in the range of 0-40 kHz of the sensor showed a different frequency shift of the imprinted layer, as seen in Fig. 2.12. At the initial range of the MIP layer height, the frequency shift of the sensor increased remarkably and gained the plateau region in the range of 20-40 kHz layer height. It was probably due to the recognition sites were not only created at layer surface but also generated through the layer. At the initial range of the layer thickness, the completion of template washing can be occurred and the recognition sites produced can be consequently inserted by template in rebinding experiment. Hence, the frequency shift of the sensor increased with an increase in the layer height.

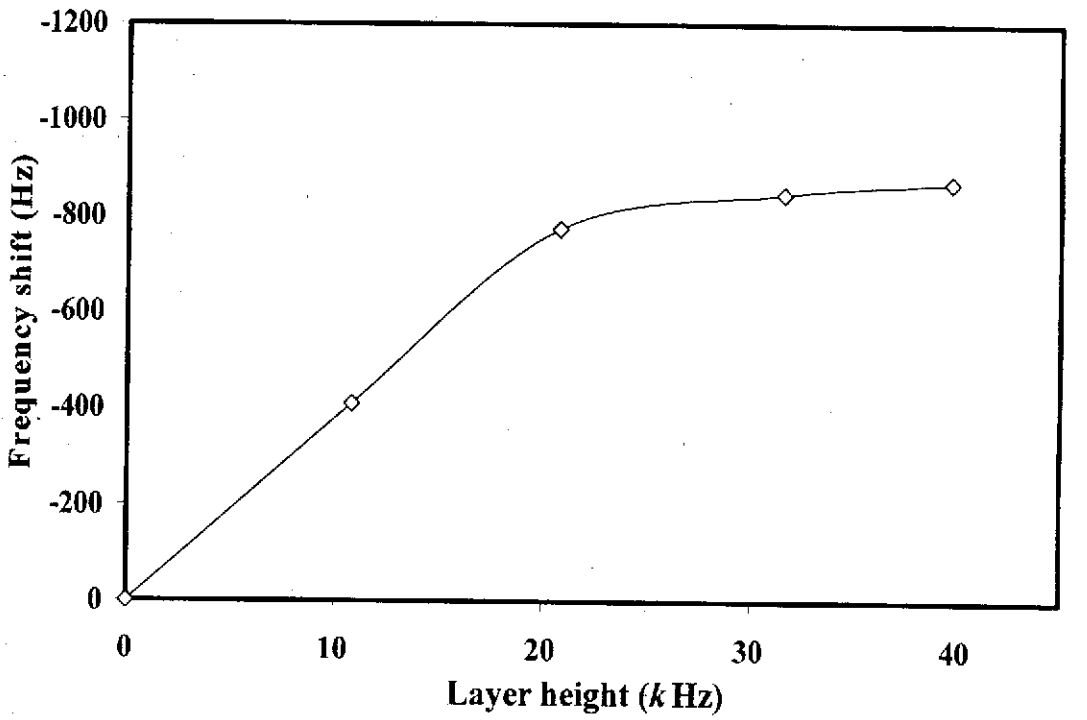

Fig. 2.12. Effect of the imprinted layer height on the frequency shift of the TCAA imprinted coated QCM exposed to the TCAA at concentration level of 100 μg l^{-1}.

In contrast, even though there were more imprinting template amounts incorporated into the bulk layer at higher layer height. The template washing process could not

remove all of the templates embedded in the polymer matrix. There were still same template molecules that remained in the layer, and those recognition sites containing with template could not be refilled with the template during the rebinding measurement. Therefore, the steady state of the signal response was observed with an increase in the layer height in the range of 20-40 KHz. And this sensor showed a reasonable analysis time with a steady response of the sensor was achieved within 20 min.

2.2.4.3. The effect of measurement background solution on frequency shift of TCAA-MIP-QCM sensor

There is difficulty of the prepared sensor to avoid from contamination of ionic species existing in real water sample especially from various inorganic acids. To better understand how these compounds affect the sensor response, the effects of inorganic salts in running solution were investigated. In general, different pH and types of ionic moieties gave different swelling phenomenon of the MIP film and difference in signal response of the sensor might be subsequently obtained. The prepared MIP coated sensor was therefore exposed to 10 mg l^{-1} TCAA in various buffer solutions at pH 1, 4 and 7 (acid solutions). The signal response of this sensor in those solutions was shown in Fig. 2.13. It was found that the MIP coated QCM sensor expressed different frequency responses at different pH of background solution. The frequency changes of 482, 105, 210 and 374 Hz were represent signal responses of the sensor in de-ionized water, 0.2 M HCl–KCl buffer pH 1, 0.2 M phosphate buffer pH 4 and 0.2 M phosphate buffer pH 7 running solution, respectively. This showed that the sensor had highest frequency response in de-ionized water comparing with the other background solutions. It may be possible for some competitive interactions from a large amount of ionized form of an acid ingredient in background solution that interfered with the functional group in the binding site and template. This could lead to the decrease in template binding and hence, frequency response of the sensor. The signal response of MIP based sensor was observed to be more affected by the HCl-KCl than phosphate buffer at the same concentration. The toughness of polymer coated on such proposed sensor in de-ionized water was also evidently revealed with the use of 24 hrs hydrated polymer in frequency response measurement compared with the same dry polymer measured in air. Their signal

responses were very close (9.965 and 9.967 Hz) and without obvious deterioration of coated polymer layer. This strength may be derived from the use of hydrophobic cross-linker, EDMA, which help prevent the serious inclusion of water molecule into the polymer layer. Ordinarily, this cross-linker creates a cross-linked imprinted polymer that is dense, inert and highly stable which contributed to the rigidity of the polymer structure. The negligible change in frequency shift of the prepared sensor after complete hydration in de-ionized water of the MIP indicated that the stability of the imprinted polymer structure generated by the EDMA-based polymer. The de-ionized water was employed as background solution for exploring the interactions between the MIP QCM sensor and HAAs in water samples. It was seen to provide the highest sensor response.

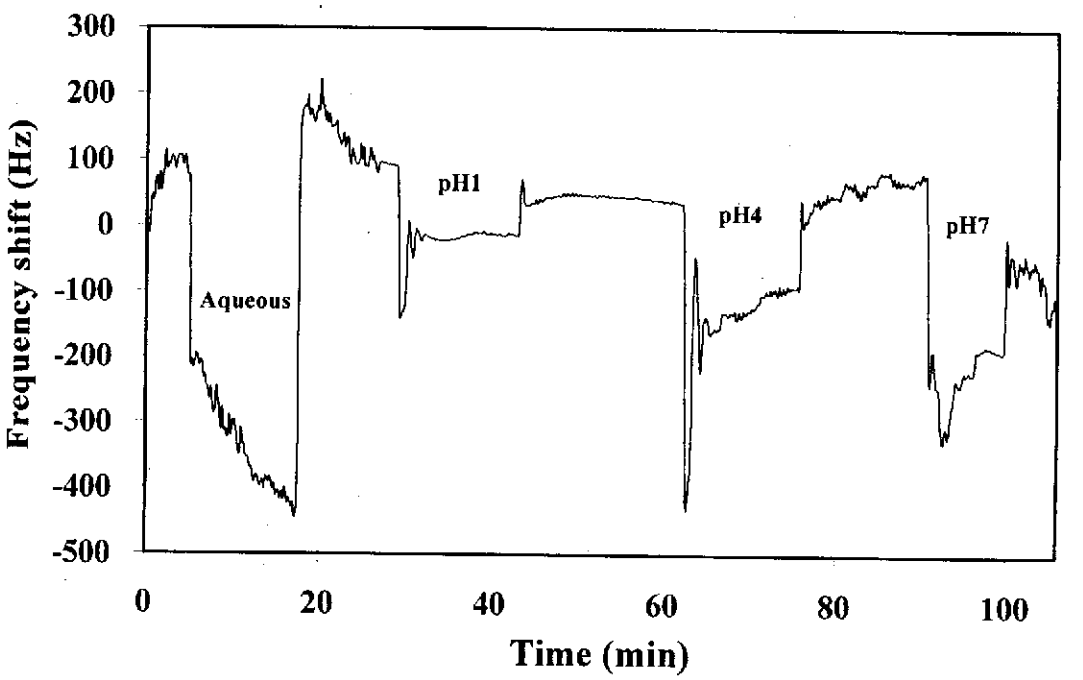

Fig. 2.13. Effect of pH of solution on frequency shift of TCAA-imprinted poly(EGDMA-*co*-vinylpyridine) modified QCM sensor

2.2.4.4. The efficiency of TCAA-MIP coated QCM

A. Concentration dependence of frequency shift response of the TCAA-MIP-QCM sensor

The signal response profile of the MIP QCM sensor was manifested by exposing it with 1 mg l^{-1} TCAA solution comparing with the NIP QCM sensor. As seen in Fig. 2.14, the frequency shift of the MIP sensor dramatically declined in this TCAA solution and nearly completely returned its frequency back to the original value by washing it with pure water. In contrast, the frequency shift response of the NIP QCM sensor was negligible in this TCAA solution. It could be assumed that the imprinting process created molecular holes in TCAA-imprinted polymer which fit well with the TCAA template molecule. The inclusion process of template into the recognition site caused such considerable signal response of the QCM sensor. The change in frequency of the sensor related to the mass change of the MIP film when disclosed to TCAA solution was possibly owing to the change in the commonly water exited counter-ion as template which interacted with functional group in imprinted site of the polymer. The force guiding TCAA template into binding site of MIP was believed to come from interaction between ionized form of functional group of template, carboxylate anion, and ionized form of functional group of MIP, vinylpyridinium cation. The positive charge of imprinted cavity can induce the negative charged TCAA to come closer then interacted and ultimately included into the cavity. Besides, the results indicated that the removal of TCAA from the recognition site was possible with de-ionized water. This reversible interaction of template and MIP was possibly due to relative concentration of TCAA in water solution compared in MIP matrix.

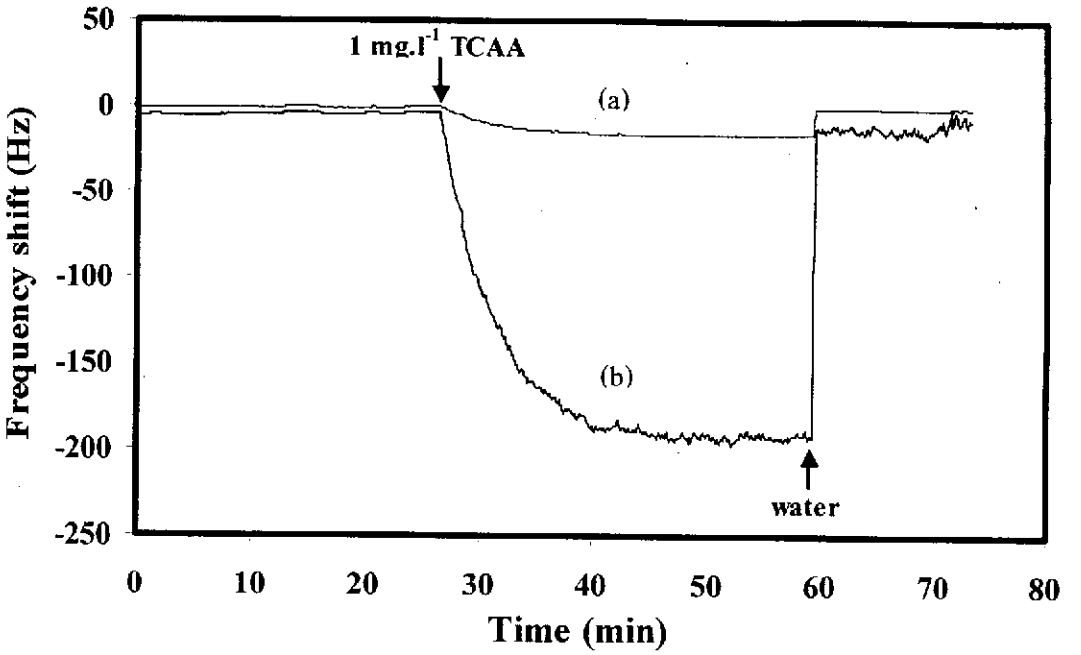

Fig. 2.14. Signal response of the QCM sensor with (a) NIP- and (b) MIP-coated electrode to TCAA at concentration level of 1 mg l^{-1}.

The signal response of the MIP QCM sensor to a series of concentration incremental TCAA solution can be seen in Fig. 2.15. At the initial range of TCAA concentration (0-50 mg l^{-1}), the results demonstrated that the frequency shift response of TCAA-MIP-QCM proportionally increased with an increase in concentration of TCAA in water. The signal response of the sensor gained a steady state when exposed with higher concentration of TCAA (100-200 mg l^{-1}). This could be due to, at initial concentration of TCAA, the binding sites was gradually filled with template molecule until the whole cavities were occupied by TCAA template at higher concentration of TCAA. This phenomenon revealed saturation of imprinted cavities of the polymer matrix with the template molecules.

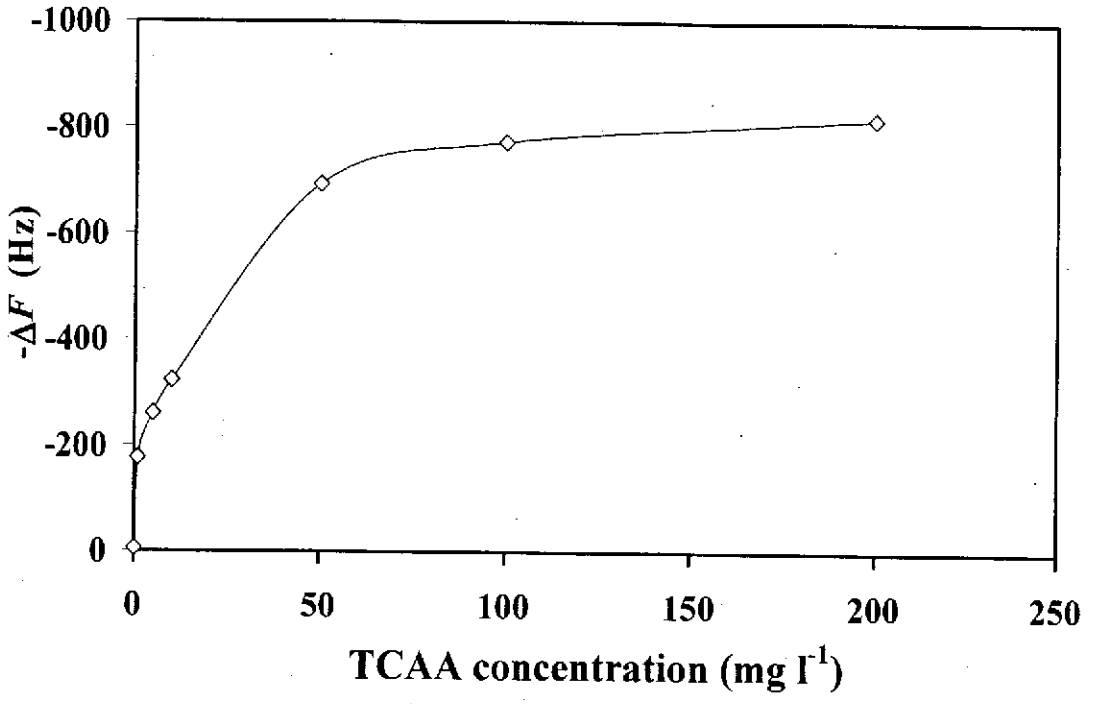

Fig. 2.15. Effect of different concentration of TCAA (0-200 mg l^{-1}) on the frequency shift response of the TCAA-MIP-QCM.

To explain the binding mechanism and behaviour of TCAA to MIP, binding parameters of imprinted polymer was approximately evaluated by using Scatchard analysis (Fig. 2.16). The Scatchard equation (Zhou, 1999) is presented as follows: $Q/[TCAA] = (Q_{max} - Q)/K_d$, where Q represents the amount of TCAA bound to the polymer, [TCAA] is the equilibrium concentration of TCAA, Q_{max} the apparent maximum number of binding sites, K_d the equilibrium dissociation constant. K_d and Q_{max} can be acquired from the slope of the straight line and the intercept of the Scatchard plot, respectively and the binding constant (K_a) value was received from the reciprocal of the K_d value. By plotting $Q/[TCAA]$ versus Q, a straight line with a dissociation constant value (K_d) of 0.094 mM (K_a = 10.60 mM^{-1}) and the Q_{max} value of 18.9 nmol was obtained. This analysis suggested unique distribution characteristic of imprinted sites generated in polymer matrix as a straight line of Scatchard plot provided only one slope in the TCAA concentration range studied.

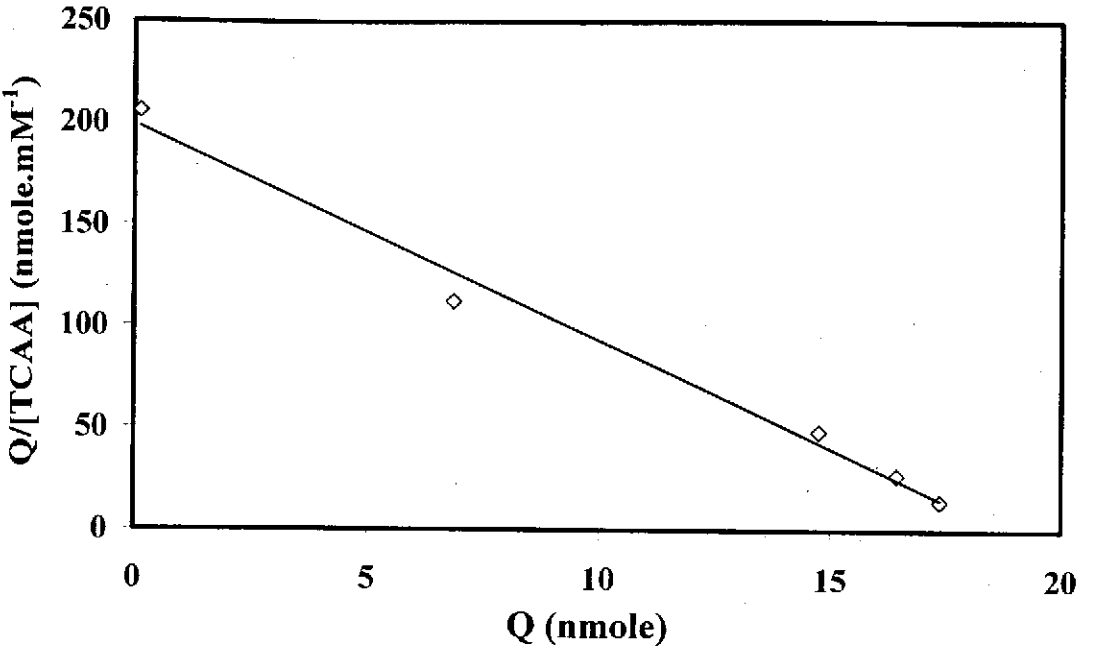

Fig. 2.16. Scatchard plot used to analyse binding parameters relative to concentration dependence of the sensor.

B. Selectivity of the TCAA-MIP-QCM sensor to template analogs

The ability of TCAA imprinted QCM sensor in binding with TCAA analogs was investigated using five structurally related TCAA compounds such as DCAA, MCAA, TBAA, DBAA and MBAA. The effect of substituted halogen atom in haloacetic acids was examined by comparing the signal response of the sensor to TCAA and its analogs with two non-related TCAA compounds (non-haloacetic acids) such as acetic acid and malonic acid. To gain insight in how imprinted QCM sensor response to TCAA analogs and non-haloacetic analogs, various parameters (K_a and Q_{max}) concerning binding process of MIP QCM sensor and analytes were collected and showed in Table 2.1. The results revealed that between the five HAA analogs and non-haloacetic acid analogs (acetic acid and malonic acid), the former group fit better to the TCAA-imprinted cavity. However, their ability in locating into TCAA-imprinted cavity was lower than that of the TCAA template. The affinity of each analog toward the TCAA-imprinted site was examined by measuring the cross-reactivity (CR) as can be seen in Table 2.1 which was defined as the ratio of the frequency shift measured at EC_{50} for analog to that of

TCAA. It was clear that CR value of five HAA analogs was lower than that of the template. Unexpectedly, non-haloacetic acids (malonic acid and acetic acid) were cross-reacted with TCAA-MIP-QCM, but in a much lower degree than that observed for HAA analogs. The selectivity of the TCAA MIP-QCM for five structurally related HAA analogs and non-structurally related acid analogs can be ranked as TCAA>DCAA>TBAA>DBAA>MBAA>MCAA> malonic acid > acetic acid. From the selectivity profile acquired, the tri- or di-substituted HAAs showed higher cross-reactivity than that of mono-substituted HAAs, In contrast, no difference in the cross-reactivity of MIP sensor to chloro-HAA and bromo-HAA analogs with the same degree of halogen substitution was observed. The recognition ability of the TCAA analogs by the TCAA-MIP-QCM sensor was presumably due to interactions of the carboxylate anion of template and the binding site cation dominated in a recognition mechanism in terms of size and shape concurrently. The analogs constituted of different halogen atom (type and number) caused their different molecular size and shape and consequently different binding behaviour. The results demonstrated that CR value higher than 80% measuring with TCAA-MIP-QCM can receive four out of six HAAs (e.g. DCAA, TBAA, DBAA and MBAA). The CR value between 70% and 60% matches one out of six HAAs (e.g. MCAA) while non-structurally related analogs, malonic acid and acetic acid, showed the CR value about 20%. This results suggested that there might be comparable competition mechanism from analogs anion to contend against template and TCAA-MIP ion pair. For each analog to fit into the imprinted cavity, it depends on the type and number of halogen atom located in the molecule. It seemed the analogs which composed of similar type and number of holagen atom as template could possibly gain a good cross-reactivity with the MIP-QCM sensor. While the MIP-QCM sensor contrastly showed very low specificity to analogs with no halogen atom constituted in molecule. Reasonably, although the TCAA-MIP QCM sensor displayed the cross-reactivity with both other HAAs analogs and non-haloacetic acid substances, the TCAA absolutely had preference over the all other analogs in terms of re-binding owing to produced recognition site principally resembled with TCAA template.

Table 2.1

Binding constant (K_a), site population (Q_{max}) and cross-reactivity related to TCAA (CR) of the TCAA-MIP-QCM responding to TCAA and analogs (n = 3)

Substrate	K_a (mM^{-1})	Q_{max} (nmol)	CR[a] (%)
TCAA	10.6	18.9	100
DCAA	7.0	14.1	80
MCAA	4.0	13.2	66
TBAA	6.4	13.8	84
DBAA	5.1	14.1	84
MBAA	4.3	13.2	83
Acetic acid	2.5	10.6	18
Malonic acid	2.2	12.6	20

[a] CR is the ratio of the frequency shift measured at EC_{50} for analog to that of TCAA. EC_{50} is the analyte concentration for which HAA binding to MIP is inhibited by 50%

C. Analytical characteristics of the TCAA-MIP-QCM in the QCM-based assay of HAAs

Concentration of HAA in the range of 0.1 to 100 mg l^{-1} in de-ionized water was employed as sample solution to explore analytical characteristics of the TCAA-MIP-QCM in the QCM-based assay of HAA. The acquired data are summarized in Table 2.2. The calibration plot derived from the frequency shift response ($-\Delta F$) dependency of the sensor to each concentration of analyte afforded comparable results for analysis of TCAA and other five HAA analogs both individually spiked and altogether mixed (see Fig. 2.17). There was a proportional relationship between frequency shift responses of the MIP-QCM sensor against the logarithm of concentrations (log C) of TCAA and analogs (individually) and the mixture of total six HAAs. A reasonable good correlation coefficient (R_2) value obtained for all analytes were in the range of 0.986-0.997 supplementary with the equation shown for each analyte in Table 2.2. The calculated EC_{50} value of 4.5 mg l^{-1} and about 20 mg l^{-1} was represent for TCAA and for the other five HAAs, respectively (see Table 2.2). This parameter was expressed as the concentration of analyte

which was able to inhibit 50% binding of HAA to MIP. The limits of detection (LOD) calculated on the basis of $3S_b/m$, where m is the linear calibration and S_b estimated as the standard deviation of the signal response for HAAs by MIP sensor, were in the range of 20 and 60 μg l^{-1} for the various HAAs. TCAA and DCAA revealed the detection limits in the mid to low μg l^{-1} range. The World Health Organization (WHO) has set a maximum permissible concentration level for DCAA and TCAA at 50 and 200 μg l^{-1}, respectively. Therefore, for the consumer health safety reason, the domestic water samples must not contaminate with these HAAs at concentration beyond these standard values. From the LOD results gained, TCAA-MIP-QCM sensor can definitely detect and measure DCAA or TCAA at lower concentrations than the maximum permissible concentrations. In addition, the LOD values of TCAA or DBAA obtained from utilizing this MIP QCM sensor were lower than those in the published literature using the other signal acquiring systems (i.e., conductivity or amperometry methods) as shown in the Table 2.3.

Table 2.2

Analytical characteristics of the TCAA-MIP-QCM in the QCM-based assay when the QCM-based assay is conducted for a HAA(s) concentration ranging from 0.1 to 100 mg l^{-1} in de-ionized water (n=3)

Compound	Equation	R^2	EC_{50} (mg l^{-1})
TCAA	$-\Delta F = -326.47\log(C)-102.4$	0.984	4.5
DCAA	$-\Delta F = -318.72\log(C)-109.8$	0.990	15
MCAA	$-\Delta F = -289.75\log(C)-148.7$	0.997	19
TBAA	$-\Delta F = -312.83\log(C)-119.6$	0.986	20
DBAA	$-\Delta F = -316.47\log(C)-140.8$	0.992	23
MBAA	$-\Delta F = -292.70\log(C)-144.5$	0.996	25
Six HAAs[a]	$-\Delta F = -559.40\log(C)-321.7$	0.996	4.5

[a] Refers to TCAA, DCAA, MCAA, TBAA, DBAA and MBAA altogether

Analyse of MCAA or DBAA showed lower LOD than those in previous reports using HPLC–UV analyse methods. When making comparison of LOD range acquired by this MIP QCM sensor with the membrane sensor published previously using a

TCAA-imprinted poly(VPD-*co*-EDMA) embedded in polyvinyl chloride membrane, QCM sensor revealed the declined detection limits of HAAs (see Table 2.3).

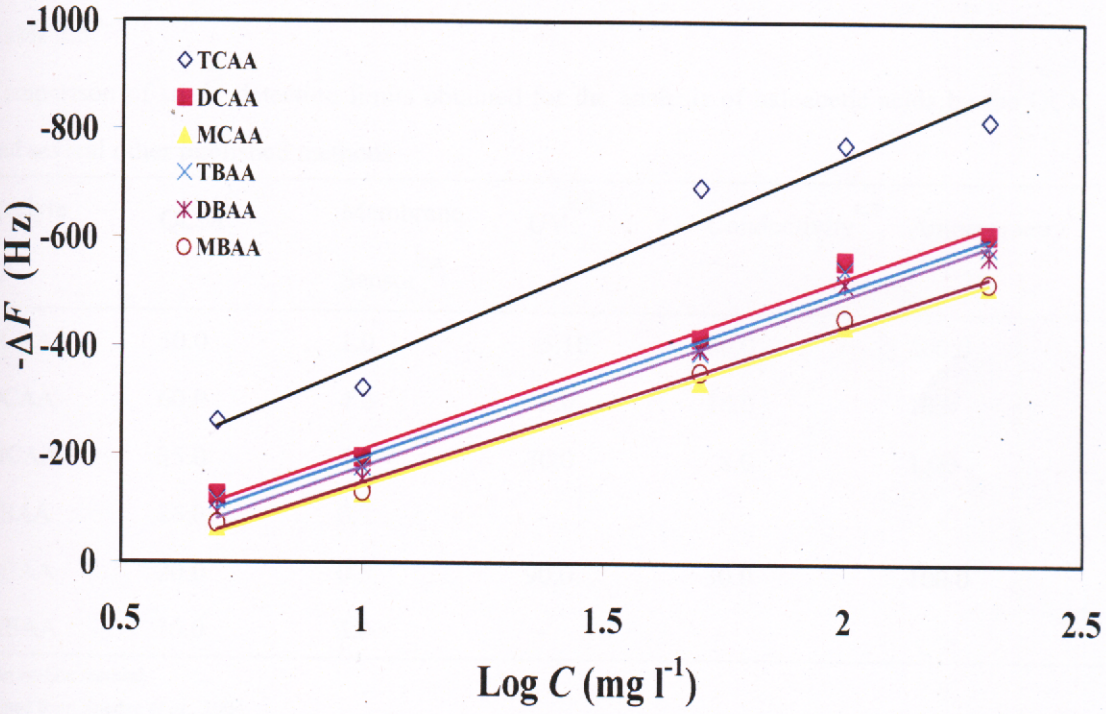

Fig. 2.17. The calibration plot of frequency shift parameter (-Δ*F*) vs. added HAA(s) for the TCAA-MIP-QCM in the QCM-based assay of HAAs. Each point represents the average of three independent measurements.

From the signal response of the sensor to each HAA, It was not able to discriminate signal response according to each analog separately. The proposed sensing method can be used only for assay signal response of total HAA. The US Environmental Protection Agency (USEPA) has regulated a maximum permissible contamination level of 60 μg l^{-1} for the five commonly haloacetic acids in water excepted for MCAA (as its solubility in water was very high and ester formed-transfer to the ether phase was definitely prohibited) in the Stage 1 of the disinfection by-product regulation. The TCAA-MIP-QCM demonstrated high specific sensitivity and selectivity in the respect with the six HAAs which suggested the possibility of using this proposed sensor as a screening and analysis tool for measuring concentrations of mixed HAA in drinking water samples. The TCAA-MIP-QCM sensor showed a good durability evidently merging with its unaffected analytical performance after storage for more than 1 month at

ambient temperature. This developed sensor has advantage, *i.e.*, an automated signal acquiring system, low-priced sensor device as well as the possibility of leading this sensor into commercial scale.

Table 2.3

Comparison of μg l^{-1} detection limits obtained for the analysis of haloacetic acids by the QCM and several other published methods

Analyte	QCM[a]	Membrane Sensor[b,a]	UV[c,d]	Conductivity[c,d]	Amperometry[c,d]
TCAA	50.0	1.0	5.10	80.0	100.0
DCAA	60.0	4.2	8.0	16.0	10.0
MCAA	35.0	4.2	70.0	8.0	1.00
TBAA	26.0	0.2	-	-	-
DBAA	20.0	0.5	90.0	30.0	100.0
MBAA	30.0	5.0	-	-	-

[a] An on-line method.
[b] Cited from Suedee *et al.*, 2004.
[c] Cited from Zielinska *et al.*, 2001.
[d] Used in the conjunction with liquid chromatography.

D. Analysis of drinking water samples

Real-life samples, which normally containing HAA group, were subjected to analysis by this developed QCM-based assay. Two brands of easy affordable commercial bottled drinking water received either from a local store or supermarket and a domestic tap water with home water treatment system were put through analysis by this method. Water samples measuring with recommended method of USEPA for HAAs, LLE-GC-ECD method, revealed only TCAA at concentration levels of 0.8, 1.0 and 1.1 μg l^{-1} contained in the bottled-water sample from a supermarket, the bottled-water sample from a local store and domestic tap water with home water treatment system, respectively. The results showed the lower HAA contents in the analysed water samples than the detection limit of the proposed sensor

manifested in this present study. The sub μg l^{-1} concentration of HAAs mixture contaminated in the real-life water samples was therefore not able acquiring from this studied QCM sensor.

In order to investigate the performance of this QCM sensor in terms of analyte recovery, the real-life water samples spiked with two different concentrations of TCAA (0.1 and 10 mg l^{-1}) or with the mixtures of six HAAs standard solution (0.02 and 2 mg l^{-1} of each, total 0.12 and 12 mg l^{-1}, respectively) were subjected to analysis by QCM sensor. The corrected concentration of HAA in real-life samples was acquired by making calculation from a calibration curve creating by pre-analysis of TCAA (or total six HAAs) contained deionised water in concentration between 0.01 and 50 mg l^{-1}. The data analysed by this QCM sensor for HAA in spiked water samples are demonstrated in Table 2.4.

Table 2.4

Analysis data for HAAs spiked in two brands of commercial bottled water and a manicupal tap water with home filtration system by the QCM-based assay

Compound/spiked concentration	Measured[a], mg l^{-1} after adding HAAs (% recovery)	
	Bottled water from supermarket	Bottled water from local store
TCAA 0.1 mg l^{-1}	103 ± 0.9	97 ± 5.3
TCAA 10 mg l^{-1}	102 ± 1.4	99 ± 1.5
Total six HAAs[c] 0.12 mg l^{-1} (0.02 mg l^{-1} each)	102 ± 2.6	99 ± 1.9
Total six HAAs[c] 12 mg l^{-1} (2 mg l^{-1} each)	101 ± 1.4	99 ± 1.3

[a] Expected concentrations are amounts added plus the amounts already present in the water sample (mean ± R.S.D, $n = 3$)

[b] With home water treatment system.

[c] Total six HAAs refers to TCAA, DCAA, MCAA, TBAA, DBAA and MBAA altogether.

Table 2.4 (Continued)

Compound/spiked concentration	Measured[a], mg l^{-1} after adding HAAs (% recovery)
	Domestic tab water[b]
TCAA 0.1 mg l^{-1}	104 ± 1.3
TCAA 10 mg l^{-1}	102 ± 2.9
Total six HAAs[c] 0.12 mg l^{-1} (0.02 mg l^{-1} each)	103 ± 5.4
Total six HAAs[c] 12 mg l^{-1} (2 mg l^{-1} each)	97 ± 1.7

[a] Expected concentrations are amounts added plus the amounts already present in the water sample (mean ± R.S.D, n = 3)
[b] With home water treatment system.
[c] Total six HAAs refers to TCAA, DCAA, MCAA, TBAA, DBAA and MBAA altogether.

It was found that the sensor expressed recovery percent in the range of 97-104% and %R.S.D. values less than 5.3% were achieved from analysis. The results implied the promising reproducibility and precision of the assay developed with the proposed sensor for the analysis of HAAs in real-life drinking water samples.

2.3. Trichloroacetic Acid Imprinted Polypyrrole Modified Quartz Crystal Microbalance Sensor

2.3.1. Objective

To evaluate the use of electrochemically synthesized polypyrrole imprinted with template trichloroacetic acid as sensitive layer onto the surface of quartz crystal microbalance electrode for analysis of haloacetic acids in drinking water.

2.3.2. Method

2.3.2.1. Immobilisation of TCAA-imprinted polypyrrole on the surface of the transducer

The immobilisation of TCAA-imprinted polypyrrole on surface of the QCM transducer was performed by means of a Coulostat at room temperature (25±1 ^{o}C). For this purpose, the electropolymerisation of pyrrole was conducted on Coulostat galvanometer at a current density of $2x10^{-1}$ μeq sec^{-1} for 50 s in an aqueous solution containing 0.1 M pyrrole and 0.1 M TCAA, under a nitrogen atmosphere. The non-imprinted polymer (NIP) films, which were employed as controls, were prepared in the same manner as the MIP films but using 0.25 M KCl instead of 0.1 M TCAA for improving electrical sensitivity in NIP solution. The coated electrode was subsequently washed with 5 portions of 50 ml de-ionized water for at least 3 h to extract the template molecules.

2.3.2.2. Piezoelectric quartz crystal microbalance-analytical detection of analyte

The coated quartz electrode was mounted in a self-made measuring cell with a 250 μl volume (Fig 2.3B). The quartz crystal was in contact with the liquid on one side only. The 100 ml of sample solution was pumped sequentially through a thermostat set at 25°C and was passed into the measuring cells which contained the quartz sensor. The flow rate of the liquid was kept constant at 2 ml min^{-1}. The measurements of sample solution and standard were made on a network analyser with home-built oscillator circuits and self-programmed processing software. For measurement of each test solution, the frequency of the imprinted polypyrrole polymer on QCM electrode was recorded in parallel experiments with the corresponding non-imprinted polypyrrole polymer. The response of sensor exposed to a solution of the analyte was reported as frequency shift response ($-\Delta F$) which is the difference between the values of frequency shift of the MIP electrode and frequency shift of the NIP electrode. Various concentrations of standard TCAA and analogs solution (0.1 mg l^{-1} to 100 mg l^{-1}) were measured.

The effects of various experimental parameters (polymer layer thickness, medium pH and electrolyte concentration) on rebinding properties and sensing performance of the TCAA-MIPpy-QCM were investigated. Calibration data for the TCAA-MIPpy-QCM sensor was obtained using concentrations of standard TCAA and analogs ranging from 0.1 mg l^{-1} to 100 mg l^{-1}. Every measurement was carried out in triplicate.

2.3.3. Material and Equipment

2.3.3.1. Material

Polydimethyl-siloxane and hardener (Sylgard 184) were obtained from Dow Corning Corporation (MI, USA).

Trichloroacetic acid (TCAA) was purchased from Merck K.G. (Darmstadt, Ger-many). Dichloroacetic acid (DCAA), monochloroacetic acid (MCAA), dibromoacetic acid (DBAA), monobromoacetic acid (MBAA), tribromoacetic acid (TBAA) and malonic acid were obtained from Fluka Chemie AG(Buchs, Switzerland).

Analytical grade pyrrole was purchased from Fluka Chemie AG (Buchs, Switzerland) and its chemical structure is displayed in the Fig. 2.18.

Fig. 2.18. The chemical structure of conducting monomer used to prepare polypyrrole film

Ammonium persulfate was the analytical grade and purchased from Ajax FineChem (Auckland, New Zealand).

All solvents used in this work were analytical grade and were dried with 4 A pore sized molecular sieve before use. Working standard solutions were prepared daily.

All chemicals for preparing buffer solution (K_2HPO_4, NaH_2PO_4, NaCl, HCl and KCl) were analytical grade and were obtained from Merck (Darmstadt, Germany).

2.3.3.2. Equipment

Atomic force microscope (AFM) (Digital Instru-ments Inc., Santa Barbara, CA) (Fig. 2.19) using a Nanoscope III Scanning tunnel microscope was used to inspect the morphology of deposited film. AFM (Digital Instruments, CA, USA) with a Nanotec Electrinica WSxM scanning probe microscopy software version 3.0 Beta 8.1 (Digital Instruments, CA, USA) was utilized to determine the thickness of the films scratching with a needle and measuring depth of the scratches.

Ismatec peristaltic pump (MCP-Process Series, Ismatec SA, Wertheim-Mondfeld, Germany) was used to drive the sample solution into the flow cell (Fig. 2.20).

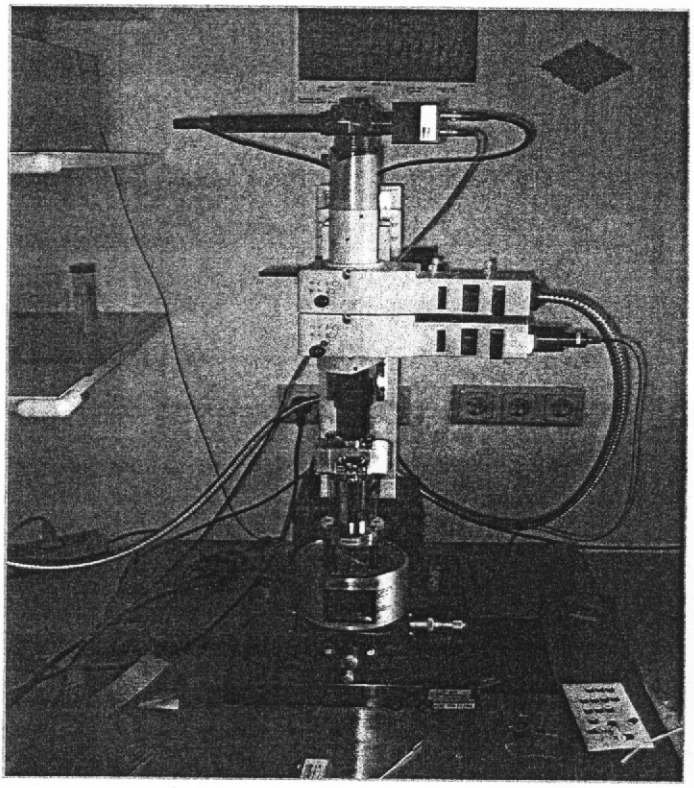

Fig. 2.19. Atomic force microscope (AFM)

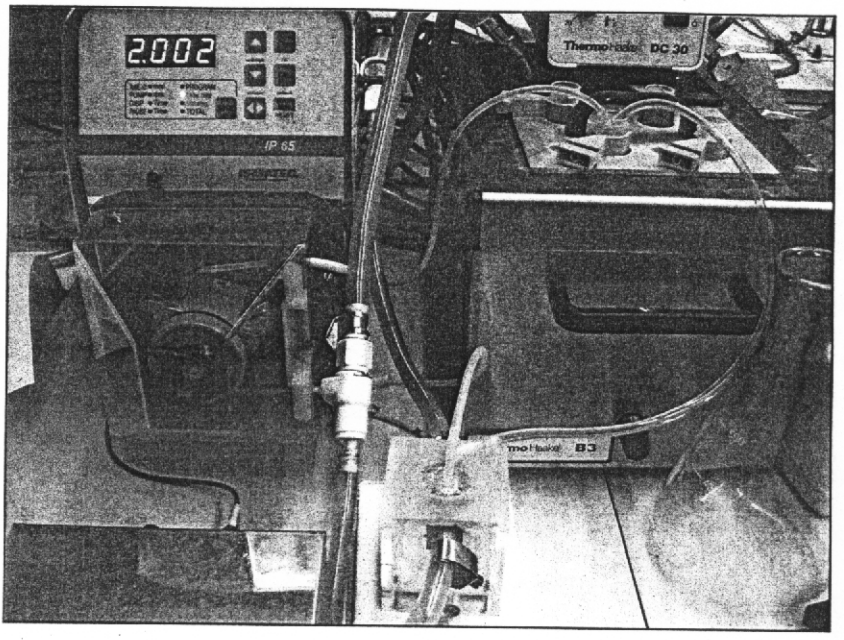

Fig. 2.20. A MCP-Process Series Ismatec peristaltic pump

A RF network analyser (8712ET 300 KHz-1300 MHz, Agilent Technologies, Palo Alto, CA) (Fig. 2.21) was utilized to monitor output signals which read the resistance signals from the sensor array with subsequent display on the Laptop screen.

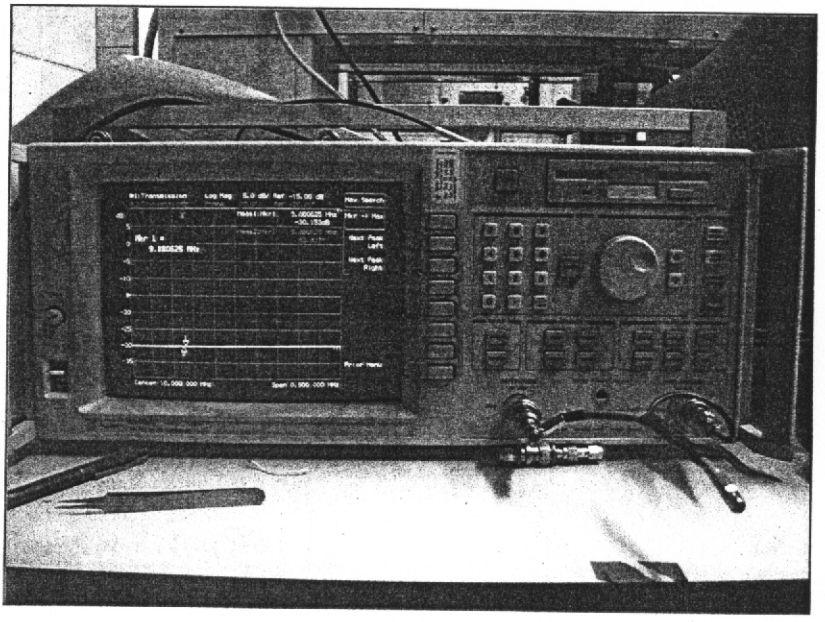

Fig. 2.21. A 8712ET RF network analyzer

2.3.4. Results and discussion

Piezoelectric QCM, that measures mass loading on the conducting electrode surface of the crystal, is one of useful transducers for analysis of analyte in a bulk solution. QCM is remarkably mass sensitivity, is relatively inexpensive and easy to fabricate on an electropolymerisable polymer material. Thus, incorporating TCAA-MIPpy with this transduction system would possibly afford an analyser that can be used for the routine analysis of HAA concentrations in drinking water. Several parameters (polymer layer thickness, monomer: template mole ratio, medium pH, electrolyte concentration) can affect the rebinding property and sensing performance of the TCAA-MIPpy QCM transducer. Thus those factors were verified before determining in the interaction of the prepared TCAA-MIPpy film with the TCAA analyte.

2.3.4.1. The MIP-based electrode optimization of synthesis condition and polymer composition

Signal transduction property of the sensor firstly based on the nature of polymer prepared. There are many parameters can be used to control the polymer characteristics, i.e. current density and polymer composition. In order to find the promising polymer layer having a good recognition property, it is necessary to investigate each parameters how it affected the signal response of the sensor. Effect of current density used to deposit polymer layer onto electrode surface can be seen in Fig. 2.22.

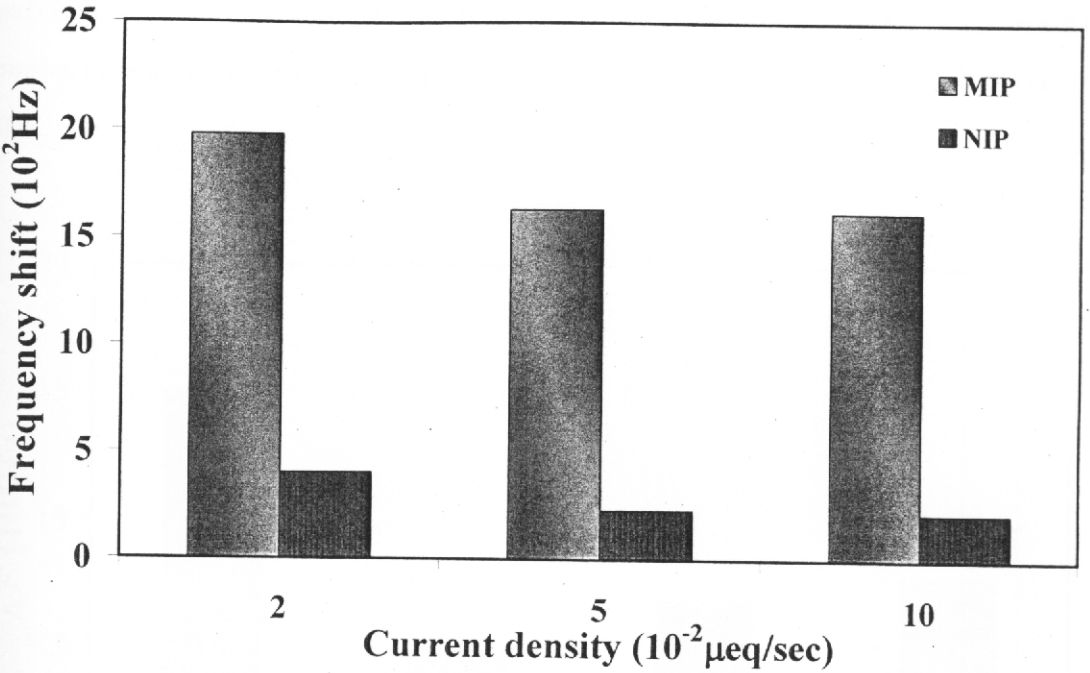

Fig. 2.22. Effect of current density in deposition process of polypyrrole on the frequency shift

It was found that the higher current density employed the lower frequency shift response of the electrode was received. It was assumably because the polymer used to prepare sensing layer was one type of conducting polymer. Its structure can be altered according to density or concentration of current. At low current density, the power of electrical energy was enough to form polymer and did not change the polymer structure to the overoxidized state (Albano and Sevilla, 2007). It was still in oxidized state which had positively charge backbone. Such structure can be induced the template closely into the binding site and produced signal transduction. In contrast, at high current density the polymer network was generated in denser fashion. Through which the template was more difficult to include, there was no charge-transfer complex occurred, the signal could not be transducted to the electrode surface.

Besides, the measurement results with the electrode imprinted with a various mole ratio of monomer and template revealed that imprinting effect, i.e. the difference of frequency shift of MIP electrode and NIP electrode, was the higher at 1:1 mole ratio of monomer : template (see Fig. 2.23). It was probably that this sensor used pyrrole as functional monomer which provides rigidity contributed component to polymer. Higher amount of this chemical was used to produce polymer layer denser of network structure. Such structure usually prohibited

entering of template molecule into the binding site. Therefore, there was no charge-transfer complex generated, frequency shift response of the sensor was then decreased (Dmitrienko *et al.*, 2006).

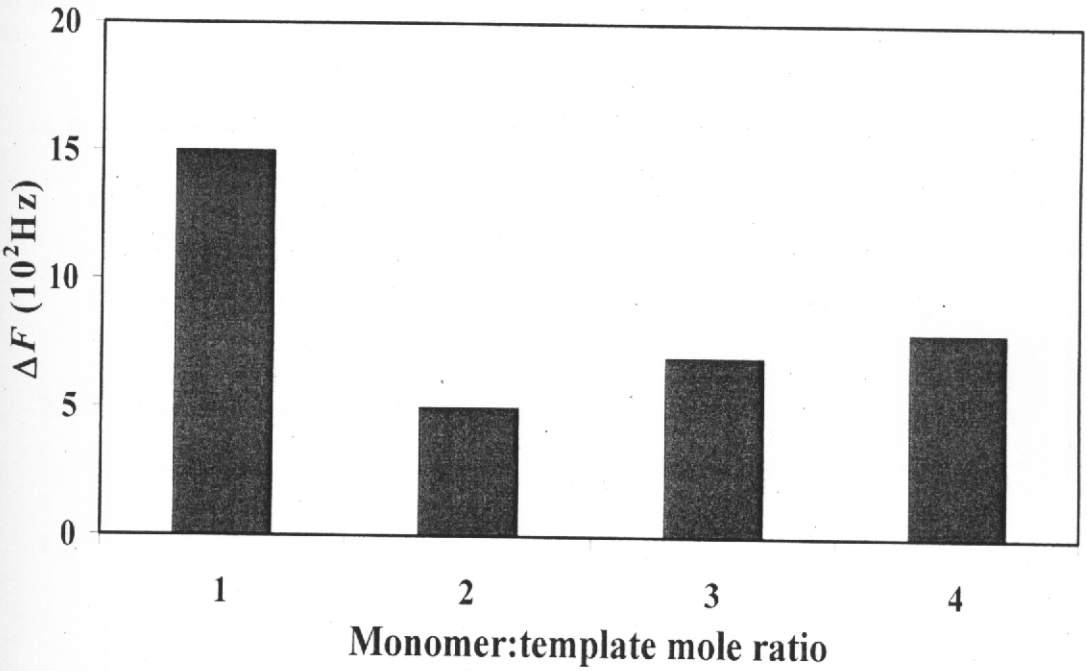

Fig. 2.23. Effect of monomer:template mole ratio on frequency shift responses of the TCAA-MIPpy coated on QCM electrode to TCAA at a concentration level of 100 mg l^{-1}.

The mechanism for the generation of the binding cavities for the TCAA template in non-cross-linked polypyrrole was proposed as follows. An oligomer of polypyrrole formed during the early stage of electropolymerisation attracted the TCAA carboxylate anions to compensate its cationic species located at the backbones. And then this repeatedly occurred until the reaction was complete in the predefined time interval. Eventually the pores or channels that had a shape and size complementary with the template molecules were produced inside the network of polypyrrole molecules.

2.3.4.2. The effect of polymer layer height on signal response of the sensor

The various layer thicknesses of the TCAA-MIPpy coated on the QCM transducer surface varied electrochemically in the range of 8-35 KHz were examined in the frequency shift response of the sensor as can be seen in Fig. 2.24.

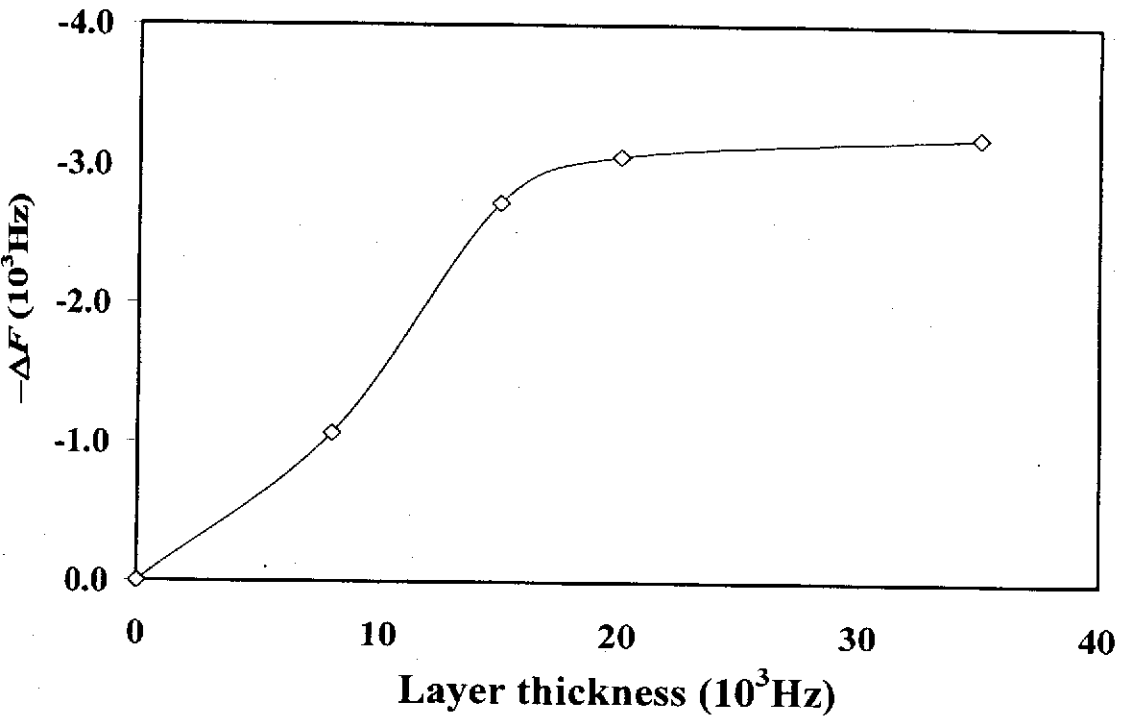

Fig. 2.24. The effect of layer thickness on frequency shift responses of the TCAA-MIPpy coated on QCM electrode to TCAA at a concentration level of 100 mg l^{-1}.

The frequency shifts increased with increase of the polymer thickness, with the greatest shift occurring between 8-15 KHz, and the shift-increase was relatively stable between 20-35 KHz. In contrast, the slightly frequency shifts with the NIP are observed. Layer height of the TCAA-MIPpy coated on the QCM was optimum at 20 KHz which equals to 800 nm thickness as calculated by the Sauerbrey equation. This would suggest that the imprint site is not only generated at the polymer surface, but also deep inside the matrix of the non-cross-linked polypyrrole layer. At the optimum layer height the imprint cavities are expected to nearly fill-up with the molecular pendents of TCAA.

2.3.4.3. The influence of ionic substances in solution background on signal response of the sensor

The ionic interaction of the function group of template and recognition site in the TCAA-MIPpy may be affected by some ionic species in the background solution resulting in QCM frequency shift response of the TCAA-MIPpy. Therefore, the effect of the pH of background solution was also investigated in pure deionised water and buffer solutions at pH 1, 4 and 7. As shown in Fig. 2.25, the TCAA-MIPpy gives the highest frequency shifts for the 10 mg l^{-1} (ppm) TCAA solution in de-ionized water, when compared to the other media. It may be because the anionic part of these substances exited in buffer solution may interfere ionic interaction between carboxylic anion of template and negatively charge oxygen bearing group along the polymer structure. In the buffer at pH 4, the interaction between anionic form of TCAA and cationic species of the MIP was strongest, compared to the other buffers. In addition, the results, in Fig. 2.25, show the interaction of TCAA with MIP can be reversible in pure deionised water.

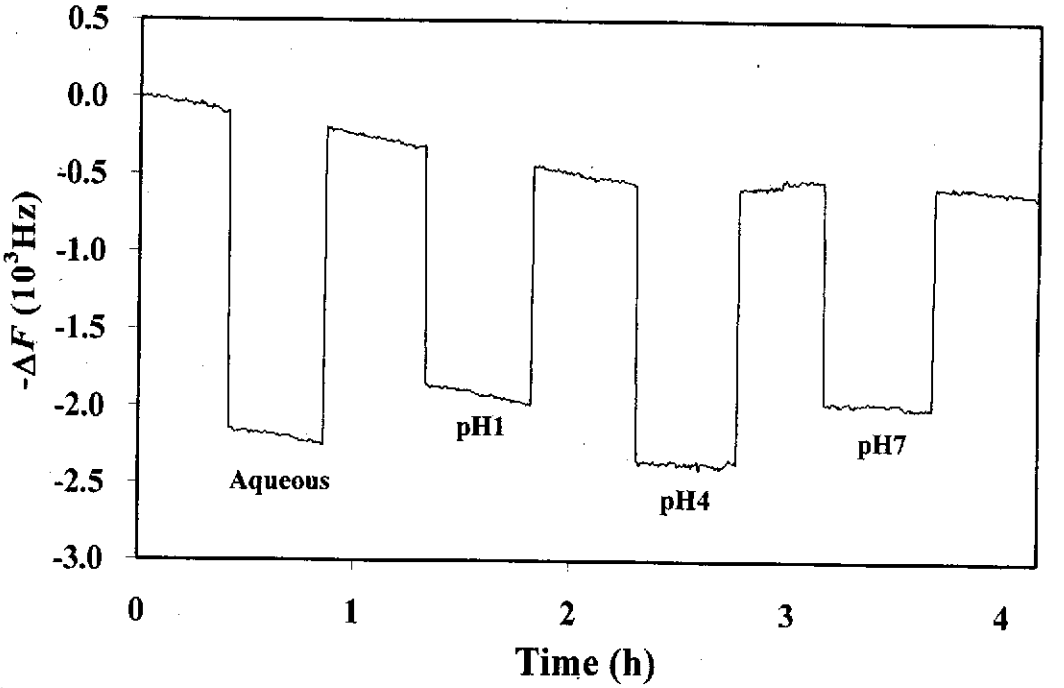

Fig. 2.25. Frequency shifts of the TCAA-imprinted polypyrrole coated QCM at various background TCAA concentrations, there is a reversible signal when washing the electrode with pure de-ionized water.

2.3.4.4. Concentration dependence of signal response of the sensor device

The dependency of the frequency shift response on TCAA and its analog concentration in the range of 0.1-100 mg l^{-1} was investigated for both the TCAA-MIPpy and the corresponding non-imprinted polymer coated electrode. Fig. 2.26 shows the TCAA-MIPpy coated electrode had a good response with the added TCAA in water sample solutions in the predetermined concentration range. The frequency shifts responses of the MIP electrode were higher as the concentration of TCAA was increased. In contrast, the non-MIP-coated electrode showed a negligible shift of frequency shift response to TCAA. This suggested that the imprinting procedures have produced cavities with a high affinity for the TCAA in MIP. Saturation of recognition sites with the template molecules occurred at the higher concentration (~ 100 mg l^{-1}) of added TCAA (see Fig. 2.26).

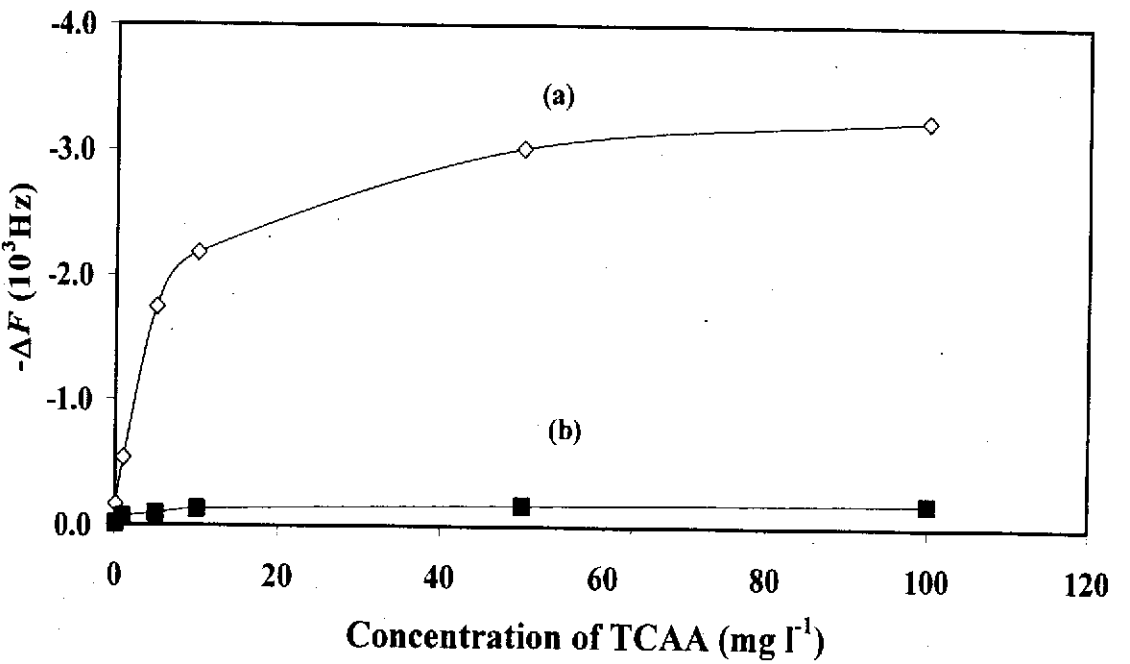

Fig. 2.26. The frequency shift of (a) the TCAA-imprinted polypyrrole coated QCM and (b) the control upon interaction with TCAA at various concentrations.

The putative binding sites of the TCAA-imprinted polypyrrole coated QCM were identified, as with the IDC studies by using non-competitive analyses method. For

this purpose, the dependency of the sensor response on concentration of TCAA and its analogs was determined in the range of 0.1-100 mg l^{-1} (ppm). Both 5 HAA analogs and the 2 non-HAA analogs (individually) in the 0.1-100 mg l^{-1} concentration range generated change in the frequency shift signal of the MIP electrode to 1 mg l^{-1} TCAA, but the level of frequency shift responses depended on the compound and its concentration, as shown in Fig. 2.27.

With the gravimetric-analytical detection method used, the amount of analyte adsorbed on the polymer layer can be estimated and binding characteristic of the imprinted layer can be obtained by Scatchard analyses studies. Table 2.5 shows the binding data for the analysis of TCAA and analogs by the non-competitive binding assay using Scatchard analysis. As can be seen, the association constant (K_a) and binding capacity (B_{max}) values were highest in the case of TCAA template when compared to those for the analogs.

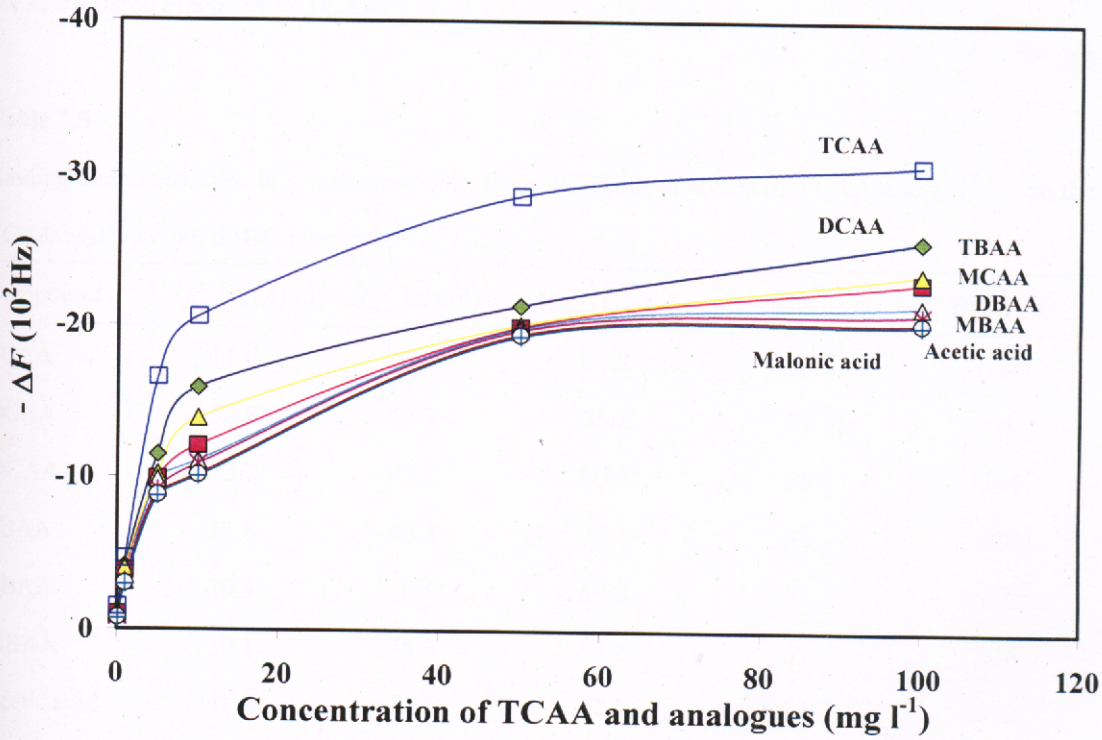

Fig. 2.27. The frequency shift response of the TCAA-MIPpy coated QCM to structurally related compounds at various concentrations.

This may be because that the recognition sites generated in the polypyrrole matrix actually have shape and size complementary with TCAA molecule. The binding data for

the analysis of TCAA and analogs on the TCAA-MIPpy coated QCM electrode suggested that the TCAA-MIPpy bound the template molecule TCAA strongly but that there is partial cross-reactivity to the 5 HAA analogs (%CR value is 20-27%), which was higher than that obtained for the non-HAA analogs (%CV <20%) (see Table 2.5). The results suggested that the non-halogen substituted compounds were poorly recognized by the MIP. Analogs with different halogen atoms and degree of substitution were recognized to varying degrees depending on their similarity to the template molecule. Also, the binding data showed a variation in the binding characteristics of TCAA template when total five HAAs were added into the TCAA solutions, and this was found to be concentration-dependent. This result suggests that the HAA analogs could compete with TCAA for the binding sites on the MIP electrode, which this will be useful for determination a group of HAAs of the TCAA-MIPpy QCM electrode. The non-structurally related TCAA compounds, malonic acid and acetic acid, showed no competitive interference for the response of the MIP-coated electrode to TCAA.

Table 2.5

Binding characteristics, IC_{50} and cross-selectivity (CR) for analyses of TCAA and analogs on the TCAA-MIPpy coated IDC electrode

Compound	K_d (μM)	B_{max} (nmol)	IC_{50} (μg l^{-1})	CR*	FS_{50} (Hz)
TCAA	11.8	61.5	64.8	100	1480
DCAA	32.8	53.2	75.2	71	1048
MCAA	33.7	47.2	80.3	65	964
TBAA	31.8	48.3	72.4	65	970
DBAA	39.4	46.5	69.8	63	938
MBAA	39.1	45.3	66.2	63	926
Acetic acid	41.1	44.5	82.5	62	912
Malonic acid	42.1	44.3	85.6	61	907

K_d is dissociation constant

B_{max} is binding capacity

IC_{50} represents the polymer content at which 50% of the polymer is blocked by the template

* Selectivity of the electrode to analyte of interest at a concentration giving IC_{50}

FS_{50} is the frequency shift at which 50% of the polymer is blocked by the template

2.3.4.5. Analytical characteristics of the sensor to TCAA and analogs

The calibration data obtained from the plot of signal response of TCAA-MIPpy versus the logarithm of concentrations of TCAA and its analogs (individually) and the mixture of total 6 HAAs are shown in Table 2.6. There is linearity in the concentration range of 0.1 to 100 mg l^{-1} (ppm) (see Fig. 2.28), with a correlation coefficient higher than 0.985. The limit of detection obtained from extrapolation of linear segments of the calibration graph was in the range of 20-40 μg l^{-1} for either TCAA or 5 HAA analogs. This LOD value for TCAA analyses by the QCM sensor is higher than that achieved with the IDC sensor, while the dynamic range obtained with the QCM was larger than that obtained with the IDC, whereas the sensor showed the lowest dynamic range when responded with template. When integrating these transducing systems with the TCAA-MIPpy thin-film the specificity characteristics of TCAA-MIPpy shown on the QCM analyses were similar to those for the CV analyses.

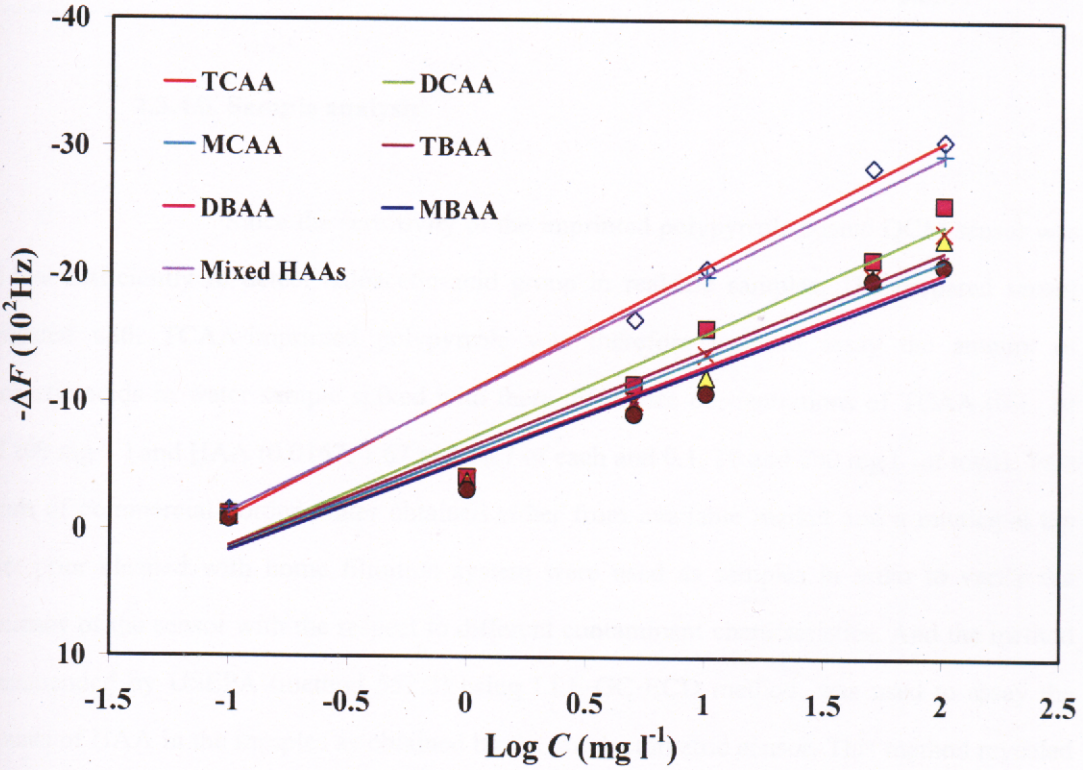

Fig. 2.28. The dependency of frequency shift response of MIPpy-coated TCAA on various concentration of TCAA, analogs (individually) and mixed 6 HAAs.

Since prepared TCAA-MIPpy integrated with QCM transduction system shows high specific sensitivity for HAA analysis in water, this TCAA-imprinted polymer material has been employed as a detection tool for analysis of HAA disinfection by-products in real-life samples.

Table 2.6

Calibration data of TCAA and five other analogs analysed by MIP sensor

Analogs	Working range (ppm)	R^2	LOD (ppm)
TCAA	0.1 - 100	0.995	0.036
DCAA	1 - 100	0.993	0.037
MCAA	1 - 100	0.995	0.038
TBAA	1 - 100	0.998	0.035
DBAA	1 - 100	0.988	0.029
MBAA	1 - 100	0.985	0.023

2.3.4.6. Sample analysis

Since the sensitivity of the imprinted polypyrrole coated QCM sensor was not low sufficiently to detect haloacetic acid group in real-life samples. The prepared sensor fabricated with TCAA-imprinted polypyrrole was therefore used to assay the amount of haloacetic acids in water sample spiked with there difference concentrations of TCAA (0.1, 10 and 100 mg l^{-1}) and HAA (0.0167, 1.67 and 16.7 of each and 0.1, 10 and 100 mg l^{-1} of total). Two brands of commercial bottled water obtained either from available market and a municipal tap water prior cleaned with home filtration system were used as samples in order to verify the efficiency of the sensor with the respect to different contaminant characteristics. And the method recommended by USEPA (method 552.2) using LLE-GC-ECD method, was used to assay the amounts of HAA in the samples as obtained by the conductometric sensor. This method revealed only TCAA at concentration levels of 0.8, 0.9, 1.0, and 1.2 mg l^{-1} in the samples contained in the bottled water sample from a supermarket, the bottled-water sample from a local supplier 1, 25 liter and municipal tap water with home filtration system, respectively. Recoveries data of

analysis are summarized in Table 2.7. As can be seen that, the sensor can recover the HAA in the range between 96 and 103% and %R.S.D. values analysed by the sensor less than 7.7% was obtained. The ability of sensor to recover template was a bit higher than that of mixed HAA spiked in all water samples. This additionally suggested the specificity of the sensor to TCAA template in real-life samples. The result demonstrates the reproducibility and precision of the assay with the use of sensor for the analysis of HAAs in drinking water samples.

Table 2.7

Analysis data for HAAs spiked in two brands of commercial bottled water and a municipal tap water with home filtration system by the QCM-based assay

Compound/spiked concentration	Measured[a], mg l^{-1} after adding HAAs (% recovery)	
	Bottled water (supermarket , 1 l)	Bottled water (local supplier, 1 l)
TCAA 0.1 mg l^{-1}	101 $\pm$ 3.7	103 $\pm$ 5.1
TCAA 10 mg l^{-1}	100 $\pm$ 0.5	100 $\pm$ 0.5
TCAA 100 mg l^{-1}	98 $\pm$ 0.3	99 $\pm$ 0.4
Total six HAAs[c] 0.1 mg l^{-1} (0.0167 mg l^{-1} each)	100 $\pm$ 1.9	102 $\pm$ 0.9
Total six HAAs[c] 10 mg l^{-1} (1.67 mg l^{-1} each)	99 $\pm$ 0.5	100 $\pm$ 0.4
Total six HAAs[c] 100 mg l^{-1} (10.67 mg l^{-1} each)	99 $\pm$ 0.2	100 $\pm$ 0.5

Table 2.7 (Continued)

Compound/spiked concentration	Measured[a], mg l^{-1} after adding HAAs (% recovery)	
	Bottled water (local supplier, 25 l)	Water filtration system (home)
TCAA 0.1 mg l^{-1}	99 ± 1.0	98 ± 7.7
TCAA 10 mg l^{-1}	98 ± 0.6	98 ± 0.5
TCAA 100 mg l^{-1}	97 ± 0.7	97 ± 0.3
Total six HAAs[c] 0.1 mg l^{-1} (0.0167 mg l^{-1} each)	97 ± 2.9	97 ± 2.9
Total six HAAs[c] 10 mg l^{-1} (1.67 mg l^{-1} each)	97 ± 0.4	99 ± 0.4
Total six HAAs[c] 100 mg l^{-1} (10.67 mg l^{-1} each)	97 ± 0.3	96 ± 0.3

[a] Expected concentrations are amounts added plus the amounts already present in the water sample (mean ± R.S.D, $n = 3$)

[b] With home filtration system.

[c] Total six HAAs refers to TCAA, DCAA, MCAA, TBAA, DBAA and MBAA altogether.